ABSTRACT

Title of Thesis: GEOTECHNICAL PROPERTIES OF COMPOST AMENDED TOPSOILS FOR USE ON HIGHWAY SLOPES

Ahmet Okan Duzgun
Master of Science, 2020

Thesis Directed By: Professor Ahmet H. Aydilek
Department of Civil and Environmental Engineering
University of Maryland

The amounts of municipal solid waste (MSW) generated in the U.S. increase every year, and about 30% of MSW generated is either recyclable or compostable. Utilization of compost-amended topsoils as a vegetative growth layer on highway slopes contributes to large volume beneficial reuse of these materials. This study examines the shear and hydraulic properties of two types of composts, biosolids and leaf compost, and their blends with a topsoil. Direct shear and consolidated-undrained (CU) triaxial compression tests were performed to obtain the shear strength parameters, which were then used to analyze the highway slope stability. Flexible-wall hydraulic conductivity tests and unsaturated hydraulic tests were performed to evaluate the saturated and unsaturated hydraulic behavior of the materials, respectively. Compost addition resulted in an increase in effective friction angle, whereas modest changes were observed in effective cohesion, total cohesion and total friction angle of topsoil. No significant change was observed on factors of safety of highway slopes by compost treatment, under both saturated and unsaturated conditions. Two shape parameters determined via digital image analysis, angularity and form 2D, correlated well with the measured effective friction angles of the materials tested. Compost treatment resulted in an increase in saturated hydraulic conductivity and the plant-available water content. Unsaturated hydraulic conductivities of all materials were comparable at the matric potential of field capacity (10 kPa), and the compost-amended topsoils experienced 1-3 orders of decrease in their unsaturated hydraulic conductivities during the drying process.

GEOTECHNICAL PROPERTIES OF COMPOST AMENDED TOPSOILS FOR USE ON HIGHWAY SLOPES

by

Ahmet Okan Duzgun

Thesis submitted to the Faculty of the Graduate School of the
University of Maryland, College Park, in partial fulfillment
of the requirements for the degree of
Master of Science
2020

Advisory Committee:
Dr. Ahmet H. Aydilek, Chair
Dr. Sherif M. Aggour, Committee Member
Dr. Dimitrios G. Goulias, Committee Member

© Copyright by
Ahmet Okan Duzgun
2020

Dedication

I dedicate this thesis to my family and Laura, for their endless love and support.

Acknowledgements

I want to thank my advisor, Dr. Ahmet H. Aydilek, for his continual guidance and support. Thank you to my committee members Dr. Sherif Aggour and Dr. Dimitrios Goulias, for their time and helps. A special thanks to Dr. Mustafa Hatipoglu for his encouragement throughout this journey.

Table of Contents

Dedication ii
Acknowledgements iii
Table of Contents iv
List of Figures v
List of Tables vi
Chapter 1 1
Introduction 2
Chapter 2 5
Materials and Methods 5
2.1 Materials 5
2.2 Methods 8
2.2.1 Shear Tests 8
2.2.2 Hydraulic Tests 10
2.2.3 Digital Image Analysis 13
2.2.4 Slope Stability Analysis 17
Chapter 3 18
Results and Analysis 18
3.1 Results of Shear Tests and Image Analyses 18
3.2 Results of Hydraulic Tests 32
3.2.1 Results of Saturated Hydraulic Conductivity Tests 32
3.2.2 Results of Unsaturated Hydraulic Tests 38
Chapter 4 48
Conclusions 48
4.1 Summary and Conclusions 48
4.2 Limitations of the Study and Recommendations for Future Research . 50
Appendices 52
Appendix A: MDOT SHA Specifications for Topsoils 53
Appendix B: Compaction and Direct Shear Tests 57
Appendix C: AIMS Analysis and Parametric Studies 66
References 74

List of Figures

Figure 1: Grain size distribution of the materials 7
Figure 2: (a) Schematic diagram (after Schindler et al., 2010a) and (b) photo of the HMS...11
Figure 3: A typical soil-water characteristic curve and the locations of FC, WP, and AWC.14
Figure 4: Aggregate Image Measurement System (AIMS) 15
Figure 5: Mohr-Coulomb envelopes for (a) T, (b) TB1, (c) TB2, (d) TL1, and (e) TL2 (solid and dashed lines represent the total and effective stress envelopes, respectively) 20
Figure 6: Direct shear results under the effective normal stresses of site condition (0.2 to 0.5 kPa) (a and d), 50 kPa (b and e), and 100 kPa (c and f) by leaf compost and biosolids amendment.....24
Figure 7: CU triaxial results under the effective normal stresses of site condition (0.2 to 0.5 kPa) (a and d), 50 kPa (b and e), and 75 kPa (c and f) by leaf compost and biosolids amendment..... 25
Figure 8: Slope stability analysis of topsoil using direct shear test parameters under saturated and 7 m - height conditions.....27
Figure 9: Correlation between angularity and friction angle by (a) B and (b) L amendment, and between the Form 2D and friction angle by (c) B and (d) L amendment 31
Figure 10: Saturated hydraulic conductivity of (a) topsoil (b) composts and compost-amended topsoils, at optimum and +5% wet of optimum contents 34
Figure 11: Effect of (a) compost and (b) gravel content on saturated hydraulic conductivity of topsoil, composts, and compost-amended topsoils.....35
Figure 12: Effect of (a) sand and (b) fines content on saturated hydraulic conductivity of topsoil, composts, and compost-amended topsoils 36
Figure 13: Effect of grain size on hydraulic conductivity by (a) biosolids and (b) leaf compost amendment 37
Figure 14: Soil-water characteristic curves of the materials tested (lines indicate fits by van Genuchten (1980) model) 40
Figure 15: Hydraulic conductivity versus volumetric water content of the materials tested (lines indicate fits by van Genuchten/Mualem model) 41
Figure 16: Hydraulic conductivity versus matric suction of the materials tested.....47

List of Tables

Table 1: Index and compaction properties of the materials tested.....9
Table 2: Summary of the direct shear and consolidated undrained (CU) triaxial test results.19
Table 3: Results of slope stability analyses.....26
Table 4: Summary of the shape property results 29
Table 5: Summary of the saturated hydraulic conductivity test results 33
Table 6: Model parameters and RMSEs for van Genuchten constrained (1980) and van Genuchten /Mualem models by estimated K_s 42
Table 7: Model parameters and RMSEs for van Genuchten constrained (1980) and van Genuchten /Mualem models using K_s measured by ASTM D5084 procedure.....43
Table 8: AWC, FC, WP and corresponding hydraulic conductivities 45

Chapter 1
Introduction

Municipal solid waste (MSW) management is a significant concern in the U.S. as the total amount of MSW increases dramatically. According to the U.S. Environmental Protection Agency (US. EPA), the total generation of municipal solid waste (MSW) in 2017 was 267.8 million tons, which is nearly 59.5 million tons greater than the amounts generated in 1990 (US. EPA, 2019). In order to decrease the need for landfill facilities, to reduce energy consumption, and for environmental protection, the management of MSW becomes essential with two main concerns: reducing the source of wastes and the reuse of wastes by recycling and composting. Maryland Department of the Environment (MDE) states that approximately 30% of MSW generated in the U.S. is compostable and defines composting as "controlled aerobic biological decomposition of organic waste material" (MDE, 2015). According to the Composting Facilities – Permitting & Operational Status of MDE, the number of permitted composting facilities is 23 with a total feedstock capacity of 520,970 tons (MDE, 2019). The amount of composted waste increases each year, and innovative reuse of compost continues to be an important issue.

In comparison to landfilling and combustion, composting generates significantly lower greenhouse gas emissions. As an example, converting 1 ton of food scraps from landfilling to composting decreases the greenhouse emissions by 0.85 metric tons of carbon dioxide equivalent (Waste Reduction Model of US. EPA, 2019). Economic aspects of composting also encourage local/state governments to seek for more extensive usage of composted materials. As the amount of MSW reduces by

recycling and composting, the need for new landfill sites decreases. Moreover, according to a report issued by the Institute for Local Self-Reliance, each ton of composted material provides twice as job opportunities as each ton of landfilled material (Platt et al., 2013).

Existing studies show that compost has various advantages over traditional topsoils, therefore, carries a potential to be used as a vegetative layer in highway slopes. Compost addition increases the soil organic matter (OM) (Intharasombat, 2005; Harrison, 2008) and stabilizes the pH (D'Hose et al., 2012; US. EPA, 2012), which are significant factors to improve the soil fertility (Eghball et al., 2004). Puppala et al. (2007) showed that mixing (50-50% by dry unit weight) an expansive clayey soil with biosolids and dairy manure compost increased the organic matter content of the soil by 3.7 and 1.3 times, and changed the pH by -0.34 and +0.3 pH units, respectively. Plant-available water content (AWC) of a soil is another significant factor, especially in terms of plant growth and erosion control, and can be increased by compost addition (Gonzalez and Cooperband, 2002; Jennings et al., 2003; Kirchoff et al., 2003; Veeresh et al., 2003). Existing work indicates that compost is a superior material when compared to topsoil for promoting vegetative growth and decreasing erosion (Faucette and Risse 2002; Faucette et al. 2007, 2009; Chaganti and Crohn 2014). In a field study conducted by Mukhtar et al. (2004), the runoff mass of the dairy manure-amended topsoil was significantly lower than that of commercial fertilizers, which could be attributed to erosion control ability of the compost.

Moreover, composted materials increase the amount of plant-available nutrients (Hartl and Erhart, 2005) and, thus, have been used for revegetation, bioremediation,

and landscaping purposes (Faucette et al., 2005; Intharasombat et al., 2007; Adugna, 2016). C:N ratio of compost typically varies between 10 to 15, and composts having a C:N ratio lower than 10 provides considerable amount of plant-available N, in both short-term and long-term, as well as other nutrients such as phosphorus (P), calcium (Ca), and potassium (K) (Sullivan, 2018).

Due to the properties and benefits mentioned above, the demand for using compost in large-scale construction projects is increasing. Several State Departments of Transportation (DOTs) have been conducting field studies to study possible use of compost in highway projects, in order to minimize erosion control and promote vegetation establishment. Likewise, there is a growing interest in using compost in lieu of topsoil as the uppermost layer of soil to support vegetation on highway slopes. Such highway projects require proper understanding of geotechnical properties of compost before any design steps are considered. However, little information exists on geotechnical properties, such as strength and hydraulic conductivity, of composts and compost-amended topsoils. Shear properties are important as they govern the stability of the slopes. Soil hydraulic properties are crucial with regard to infiltration and runoff occurrence, as well as to their relevance to pore water pressure, which, in turn, influences effective overburden stresses. On the other hand, water is essential for plant growth thus infiltration through the topsoil and subsoil is needed to minimize runoffs. Thus, effect of compost amendment on saturated and unsaturated hydraulic conductivities, as well as on soil-water characteristics need to be analyzed.

To respond to this need, a series of laboratory tests was conducted in the current study on two types of composts (biosolids and leaf compost), and compost-amended

topsoils. Direct shear and consolidated-undrained (CU) triaxial compression tests were conducted to analyze the shear properties, and digital image analysis was performed to define any possible relationship between the shear strength parameters (cohesion and angle of friction) and shape/texture properties. Slope stability analyses were conducted to observe the change in the overall highway slope stability by compost amendment under varying site conditions. Hydraulic properties under saturated conditions were investigated by running falling-head hydraulic conductivity tests in flexible-wall permeameters. Lastly, unsaturated soil hydraulic properties; relationships between the soil water content and suction (i.e., soil-water characteristic curves) and unsaturated hydraulic conductivity were analyzed by the simplified evaporation method using the HYPROP Measurement System (HMS).

Chapter 2

Materials and Methods

2.1 Materials

Biosolids compost (B) and leaf compost (L), commercially named Leafgro, were used as composted materials and Maryland Department of Transportation State Highway Administration (MDOT SHA) approved screened topsoil (T) was chosen as a control soil. B was collected from City of Aberdeen, Maryland, L was supplied from a store in College Park, Maryland, and the topsoil was gathered from a landscape company in Hanover, Maryland. Materials were placed in airtight plastic buckets and stored at the room temperature upon delivery to the University of Maryland Laboratories.

MDOT SHA specifications were considered to analyze the composted materials for their possible use on highway slopes (Tables A1 and A2 of Appendix A). Since the topsoil as well as the compost-topsoil blends can be existing or furnished materials, the MDOT SHA specifications for both conditions were considered to come up with the limits in Table A3 of Appendix A.

T, L, and B were tested for textural analysis, soil pH, and OM, per MDOT SHA specifications. While T met all three requirements, pure B only met the pH limit and L did not meet the limits for pH, OM, and textural analysis, which required preparation of topsoil-compost blends. Since geotechnical engineering properties were the main focus, textural analysis was conducted (i.e., sand, silt, and clay percentages were determiend) to make a decision on mixture percentages. Sieve analysis and SALD-2300 particle size analyzer were used to determine the sand, silt and clay percentages defined in MDOT SHA specifications (which are consistent with the ones in the United

States Department of Agriculture Soil Classification System). After several trials, blends prepared with 70% topsoil+30% compost and 85% topsoil+15% compost, all based on dry unit weights of the materials and maximized the usage of compost, were considered as the optimum blends (Table A3 of Appendix A). All materials were dried at 50°C for 72 hours before mixing. To observe the effect of water content on geotechnical properties, materials were prepared at two different water content levels, optimum compaction water content (w_{opt}) and +5% of the optimum water content (w_{opt+5}).

Measured parameters for topsoil, composts, blends and their comparison with the MDOT SHA specifications are summarized in Table A3 of Appendix A. Topsoil and compost-amended topsoils met the requirements of pH and textural analysis. Organic matter (OM) of the materials was tested per AASHTO T-267. L had the highest OM content of 61.57 ± 0.071% and B had OM content of 60.55 ± 0.781%. Although T had an OM of 4.39 ± 0.193% and remained within the specification range, the mixtures could not meet the specification. However, it should be recognized that the OM limits are developed for pure topsoils, and the limits are currently being reconsidered for highly organic materials, such as compost.

Grain size distributions of the materials determined using the AASHTO T-88 procedure are given in Figure 1. B had significant amount of gravel size (>4.75 mm) wood chips (25.1%) and the lowest fines content (5.8%). L included the highest percentage (81.9%) of sand-size particles (i.e., 75 μm-4.75 mm), and had the lowest gravel-size particle percentage (2.8%). T had the highest (49.2%) fines content (i.e.,

<75 μm). Table 1 lists the index and compaction properties of the materials tested. The plasticity index (PI) of topsoil was determined as 9.7 per ASTM D4318. Both

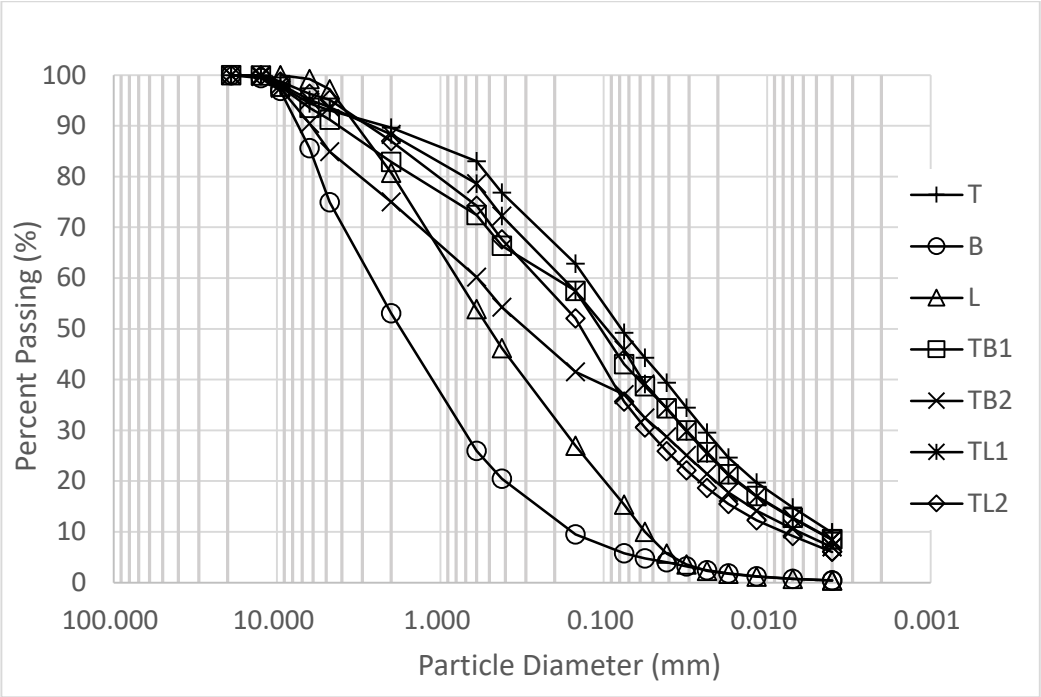

Figure 1. Grain size distribution of the materials

composts and all the mixtures were non-plastic (NP). Standard Proctor tests performed per ASTM D698 showed that the maximum dry unit weights of B and L (4.7 and 6.3 kN/m^3, respectively) were quite low compared to that of topsoil (16.8 kN/m^3), and the maximum dry unit weights of the mixtures varied between 11.3 and 13.7 kN/m^3 (Figure B1 of Appendix B). As shown in Table 1, compaction at w_{opt+5} did not cause a noticeable change in dry unit weight of the materials tested.

2.2 Methods

2.2.1 Shear Tests

Direct shear test (ASTM D3080) was performed on topsoil, composts, and amended topsoils by using the GEOTAC DigiShear–Automated Shearing System. Specimens were prepared by compacting the materials at their w_{opt} and w_{opt+5} in a shear box that is 25.4 mm in height and 63.5 mm in diameter. Each material was consolidated prior to shearing and were sheared at a displacement rate of 0.05 mm/min. The strength parameters, cohesion and friction angle, were obtained under the vertical stresses of 15, 25, 50, 75, 100, and 200 kPa.

In order to evaluate the shear properties of the blends, a series of Consolidated-Undrained (CU) triaxial compression tests was performed by using the GEOTAC Automated Load Test System and following the procedures outlined in ASTM D4767. Topsoil and compost-amended topsoils were uniformly tamped in 71.12-mm diameter and 140-mm high two-part compaction molds at their optimum water contents. Saturation (B≥0.95) was ensured prior to consolidation and shearing. Each test was performed at a strain rate of 4%/hr and under the effective consolidation stresses of

Table 1. Index and compaction properties of the materials tested

Material	Composition	Gravel (%)	Sand (%)	Fines (%)	C_c	C_u	PI	G_s	w_{opt} (%)	$\gamma_{d,max}$ (kN/m^3)	γ_d at w_{opt+5} (kN/m^3)
T	100% topsoil	7.0	43.8	49.2	1.06	33	9.7	2.58	15.7	16.8	15.8
B	100% biosolids compost	25.1	69.1	5.8	1.41	18	NA	1.22	64.8	4.7	4.7
L	100% leaf compost	2.8	81.9	15.3	0.72	16	NA	1.13	73.6	6.3	6.2
TB1	85% topsoil+15% biosolids compost	8.8	48.2	43.0	0.86	45	NP	2.43	22.1	13.6	13.3
TB2	70% topsoil+30% biosolids compost	15.1	47.8	37.1	0.55	91	NP	2.34	25.0	11.4	11.3
TL1	85% topsoil+15% leaf compost	6.4	47.8	45.8	1.0	38	NP	2.33	21.1	13.7	13.4
TL2	70% topsoil+30% leaf compost	4.8	59.5	35.7	1.24	35	NP	2.28	35.6	11.3	11.3

Notes: C_c: coefficient of curvature, C_u: coefficient of uniformity, PI: plasticity index, NP: non-plastic, NA: not applicable, G_s: specific gravity, w_{opt}: optimum water content, w_{opt+5}: +5% of optimum water content, $\gamma_{d,max}$: maximum dry unit weight

25, 50, and 75 kPa.

2.2.2 Hydraulic Tests

In order to determine saturated hydraulic conductivities of the materials, falling-head tests were performed in flexible-wall permeameters and by following the procedures listed in ASTM D5084. Samples 101.6 mm in diameter and 116.43 mm in height were compacted at their w_{opt} and w_{opt+5} using the standard Proctor effort. Saturation ($B \geq 0.95$) was ensured prior to each test, and the tests were continued under an effective consolidation stress of 20 kPa until the termination criteria outlined ASTM D5084 is achieved. A minimum testing duration of 24 hours was selected.

HYPROP Measurement System (HMS) was used to analyze the unsaturated hydraulic properties of the T, B, L, and compost-amended topsoils (Figure 2). Each sample was compacted at their optimum water content and back-saturated prior to testing. HMS is a system that collects more than 100 data points within the 0 - 100 kPa suction range, producing a high-resolution soil-water characteristic curve (SWCC). Simplified evaporation method, which uses the evaporation rather than removal of water under pressure, was used. Pressure head values at two different depths in each sample, at depths of 1.25 cm and 3.75 cm measured from the sample surface, were recorded via two tensiometers and each sample was weighed to estimate the evaporation rate, i.e., volumetric water content. Data were collected once every minute within the first hour, then once per 10 minutes until the termination of the test. The unimodal constrained model of van Genuchten (1980) was used as the retention curve fitting function and is given by:

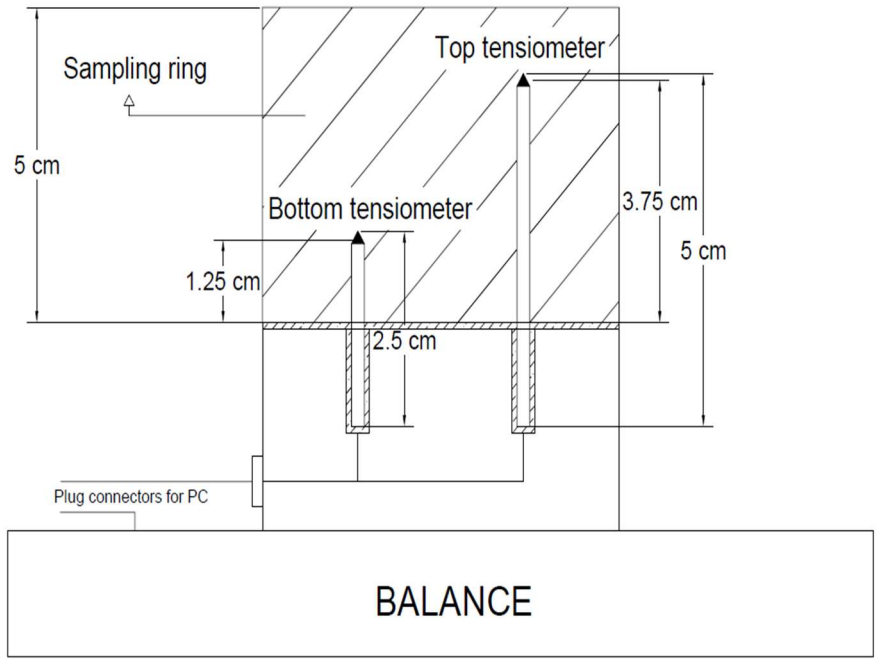

(a)

(b)

Figure 2. (a) Schematic diagram (after Schindler et al., 2010a) and (b) photo of the HMS

$$S_e(h) = \frac{\theta(h)-\theta_r}{\theta_s-\theta_r} = [\frac{1}{1+(\alpha|h|)^n}]^{1-\frac{1}{n}} \qquad (1)$$

where, S_e is the effective saturation [-], θ_s is the saturated water content [cm^3cm^{-3}], θ_r is the residual water content [cm^3cm^{-3}], α is a shape parameter [cm^{-1}] which is linked with the inverse of the air-entry pressure, n is a shape parameter [-] that is related to bending of the retention curve, and h [cm] is the pressure head.

The relationship between unsaturated hydraulic conductivity and volumetric water content was obtained and van Genuchten/Mualem model (Mualem 1976, van Genuchten 1980), was used for the conductivity fitting function:

$$K(h) = K_s(1 + (\alpha|h|)^n)^{\tau(1/n-1)}[1 - (\alpha|h|)^{(n-1)}[1 + (\alpha|h|)^n]^{1/n-1}]^2 \qquad (2)$$

where, K_s is the saturated hydraulic conductivity, and τ [-] is tortuosity.

Field capacity (FC) is the water content at which excess water has drained away and wilting point (WP) is the minimum amount of water that the plant needs not to wilt (Kirkham, 2005; Minasny and McBratney, 2018). Available water capacity (AWC) of each material was obtained as the amount of water between the field capacity (FC) and the wilting point (WP). All materials used in the current study were coarse-texture per USDA soil classification, and following the recommendations of Colman (1947), Jamison and Kroth (1958), Ratliff et al. (1983), and Huntington (2007), FC and WP were defined as the water content at soil water potential of -10 and -1500 kPa,

respectively. A schematic diagram that explains the FC, WP and AWC parameters is given in Figure 3.

2.2.3 Digital Image Analysis

Digital image analyses for T, B, L, and the blends were performed by using the Aggregate Image Measurement System (AIMS) (Figure 4). AIMS has a high resolution camera, magnification microscope, top-lighting and back-lighting which allow to obtain 2D digital images and perform texture analyses. Particles were washed and dried prior to testing and were placed in various trays for different sizes. Particles passing from #200 sieve (0.075 mm) were not used. Following the recommendations given in the AIMS Manual (2017), 50 and 150 particles were placed into the load trays for materials retaining above and passing from #4 sieve (4.75 mm), respectively, and three measurements were performed on each group of particles to minimize the effect of sampling variation.

The angularity, Form 2D (relative form of 2-dimensional images), texture, sphericity, flatness, and elongation of the particles were analyzed. Particle size ranges used during evaluation of each parameter are shown in Table 4 and equations used by the AIMS are shown below:

Angularity

$$GA = \frac{1}{\frac{n}{3}-1} \sum_{i=1}^{n-3} |\Theta_i - \Theta_{i+3}| \qquad (3)$$

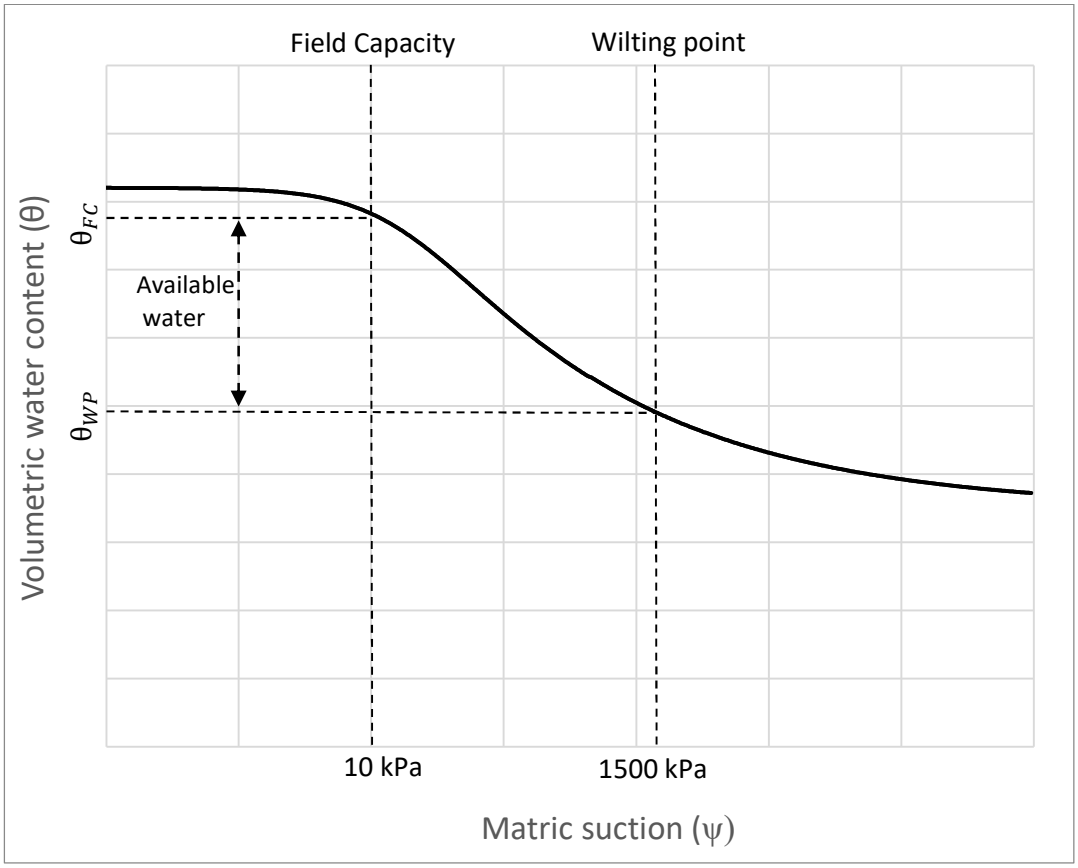

Figure 3. A typical soil-water characteristic curve and the locations of FC, WP, and AWC.

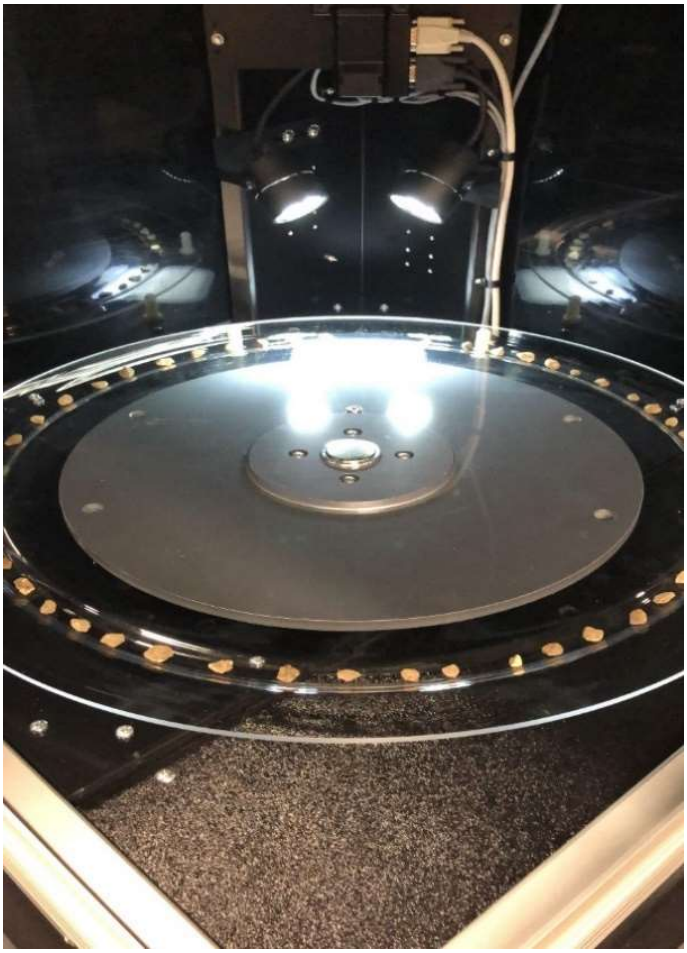

Figure 4. Aggregate Image Measurement System (AIMS)

where θ is the angle of orientation of the edge points, n is total number of points, and i refers to i^{th} point on the edge of the particle.

Form 2D

$$\mathrm{F2D} = \sum_{\theta=0}^{\theta=360-\ \theta} \left[\frac{R_{\theta+\Delta\theta}-R_{\theta}}{R_{\theta}}\right] \qquad (4)$$

where R_θ is the radius of the particle at an angle of θ, and Δθ is the incremental difference in the angle.

Texture

$$\frac{1}{3N}\sum_{i=1}^{3}\sum_{j=1}^{N}(D_{i,j}(x,y))^2 \qquad (5)$$

where n is the decomposition level, N is the total number of coefficients, i is 1,2, or 3, for three different captured images, j is the wavelet coefficient index, and (x,y) is the coefficient location

Sphericity

$$\mathrm{SP} = \sqrt[3]{\frac{d_S d_I}{{d_L}^2}} \qquad (6)$$

where d_S, d_I, and d_L are the shortest, intermediate dimension, and the longest dimensions of the particle.

Sphericity Ranges:

$0 \leq$ Low ≤ 0.5

$0.5 <$ Moderate ≤ 0.6

$0.6 <$ High ≤ 0.8

$0.8 <$ Extreme < 1.0 (cubical)

Flatness

$$F = \frac{d_S}{d_I} \qquad (7)$$

Elongation

$$E = \frac{d_I}{d_L} \qquad (8)$$

2.2.4 Slope Stability Analysis

In order to analyze the effect of compost amendment on stability of highway slopes, several analyses were performed using SLOPE/W by GeoStudio, a common software program used for slope stability. The selected slope angle was 2H:1V, the steepest slope allowed by the Maryland Department of Transportation (MDOT), and the slope heights were 7 m and 12 m. Piezometer line was defined both at the ground surface (i.e., at the slope crest level) and the bottom of the subsoil, to simulate the saturated and unsaturated conditions, respectively. Subsoil, compacted well-graded sandy soil with a natural unit weight of 18 kN/m^3, cohesion of 30 kPa, and effective friction angle of 30°, was assumed to underlie the compost. Shear parameters calculated based on effective stress analysis and derived from the direct shear and CU triaxial tests are summarized in Table 2.

Chapter 3

Results and Analysis

3.1 Results of Shear Tests and Image Analyses

The results of the direct shear tests are given in Table 2. The data indicate that there is an increase in friction angle by compost amendment. At w_{opt}, T has an effective friction angle of 36°, whereas L and B have 46° and 42°, respectively. Effective friction angles of the blends varied between those of T and composts. TL1 and TL2 have effective friction angles of 43° and 44°, respectively, and both TB1 and TB2 have an effective friction angle of 39°. T has an effective cohesion of 11 kPa and compost amendment caused an increase by 5 to 7 kPa. Compacting materials at 5% wet of their optimum contents decreased the friction angle by 2 to 6° for T, L, and L-amended blends, and increased the angle by 2 to 3° for B and B-amended blends. The effect of increasing the compaction water content (i.e., from w_{opt}, to $w_{opt\ +5}$) on effective cohesion varied from an increase of 13 kPa (L) to a decrease of 15 kPa (TB1).

CU triaxial results presented in Figure 5 show that T and TB1 have an effective friction angle of 32°, and effective cohesion of 16 and 29 kPa, respectively. TB2 has the highest effective friction angle of 47°, and an effective cohesion of 8 kPa. TL1 has the second highest effective friction angle of 45°, yet shows no effective cohesion, whereas TL2 has an effective friction of 40° and effective cohesion of 15 kPa. Results also indicate that the total friction angles and cohesions change very little by compost treatment (by 2 to 3° and 0 to 8 kPa, respectively).

Table 2. Summary of the direct shear and consolidated undrained (CU) triaxial test results

Material	Direct Shear				CU Triaxial			
	w_{opt} (%)		w_{opt+5} (%)		w_{opt} (%)			
					Effective parameters		Total parameters	
	c' (kPa)	ϕ' (°)	c' (kPa)	ϕ' (°)	c' (kPa)	ϕ' (°)	c (kPa)	ϕ (°)
T	11	36	12	34	16	32	21	32
B	8	42	11	44	NA	NA	NA	NA
L	8	46	21	40	NA	NA	NA	NA
TB1	17	39	2	42	29	32	29	30
TB2	16	39	6	41	8	47	25	27
TL1	18	43	15	40	0	45	21	30
TL2	16	44	15	41	15	40	17	32

Notes: w_{opt}: optimum water content, w_{opt+5}: +5% wet optimum water content, c': effective cohesion, c: total cohesion, ϕ': effective friction angle, ϕ: total friction angle

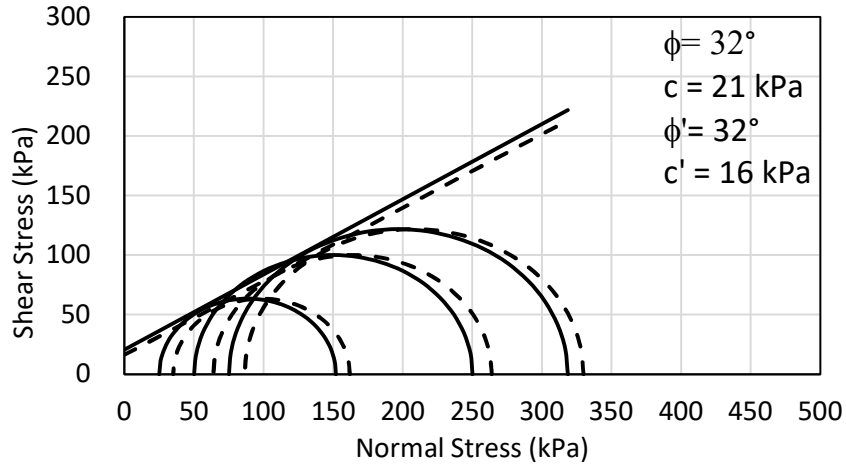

(a)

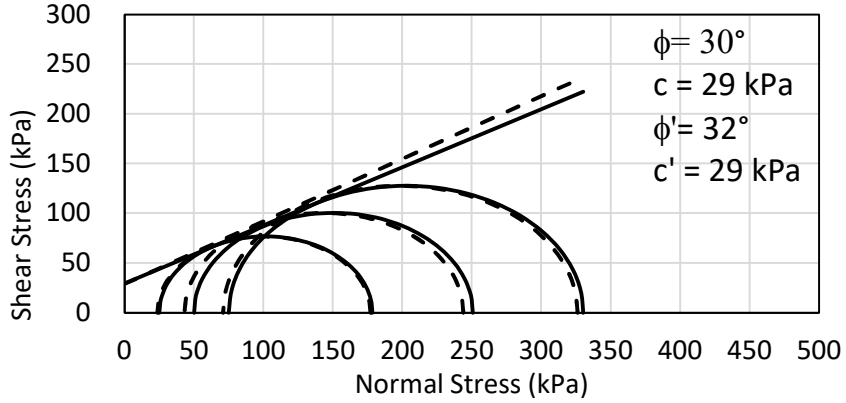

(b)

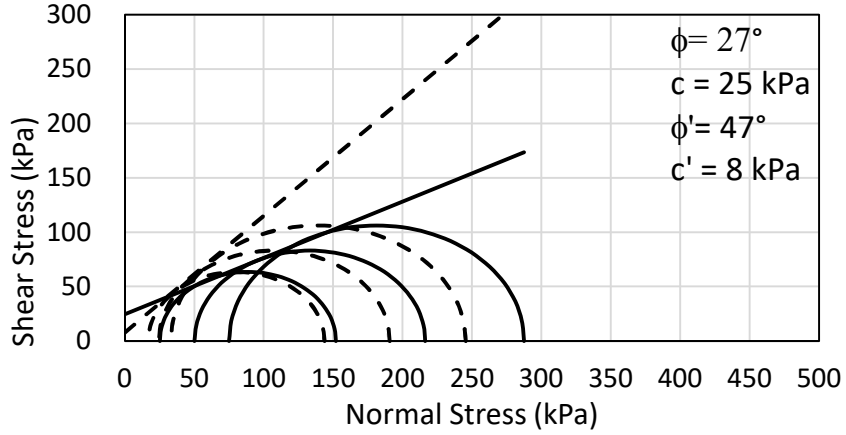

(c)

Figure 5. Mohr-Coulomb envelopes for (a) T, (b) TB1, and (c) TB2 (solid and dashed lines represent the total and effective stress envelopes, respectively)

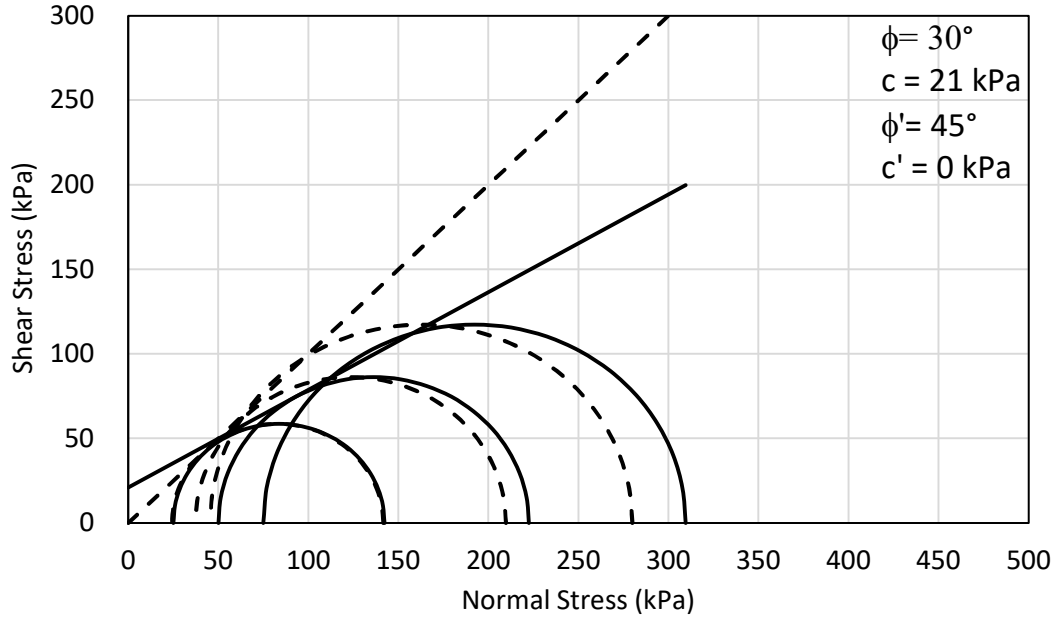

(d)

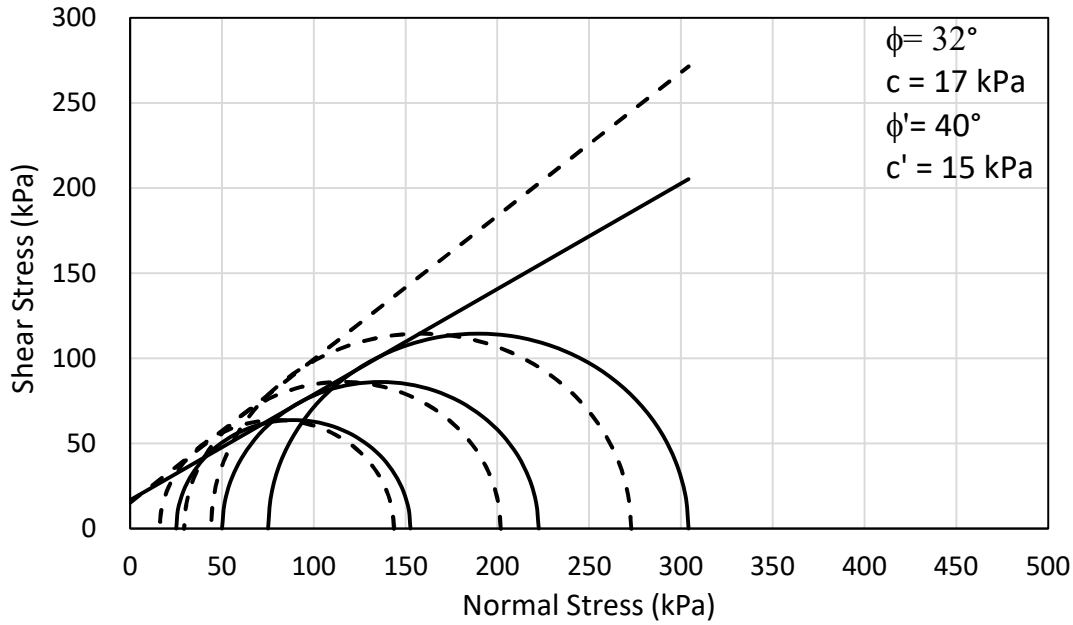

(e)

Figure 5 (cont'd). Mohr-Coulomb envelopes for (d) TL1, and (e) TL2 (solid and dashed lines represent the total and affective stress envelopes, respectively)

Bajwa and Fall (2011) found that the effective cohesion of the compost material, which consists of municipal source separated organics, varied from 4 to 5 kPa, whereas it had an effective friction angle of 45° which changed very little from the compaction water contents of 46 to 79%. Puppala et al. (2004) showed that the effective friction angle of an expansive subsoil, classified as CL per Unified Soil Classification System (USCS), increased from 3° to 23.5° upon amending with 30% biosolids compost by dry weight. The difference in degree of increase observed in past studies and the current study may be attributed to differences in compost characteristics and sources.

According to Maryland Department of Transportation (MDOT), common thickness of the uppermost vegetative layer in highway slopes is 5 cm. In-situ effective stress beneath such compost layers would vary between 0.2 and 0.5 kPa, which is significantly lower than the applied normal stresses in both direct shear and triaxial tests. Figures 6 and 7 show the change in shear stress by compost treatment under different effective normal stresses considered in both tests as well as under typical in-situ stresses.

The data show that the changes in calculated shear stresses under site conditions fluctuate, as they mostly depend on cohesion due to low (0.2-0.5 kPa) normal stresses, while the shear stress values under higher normal stresses (50-100 kPa) lead to an increase by both compost treatments. Results of direct shear tests (Figure 6) show that 15% leaf compost addition (TL1) under low normal stress increases the shear strength of T by 64% (from 11 kPa to 18 kPa). Similar observations can be made for the B treatment; shear strength increases by 55% upon 15% B addition (TB1). This trend changes as the normal stress increases. For instance, under an effective normal stress

of 100 kPa, T has a shear strength of 84 kPa, and shear strengths of TB1 and TL1 are 98 and 111 kPa, respectively.

Shear strength values obtained in CU triaxial tests under different effective normal stresses are presented in Figure 7. No clear-cut trends can be observed between shear strength and in-situ stresses (i.e., 0.2 to 0.5 kPa). Under effective normal stresses of 50 and 75 kPa, on the other hand, the trends are quite different. 15 and 30% L treatment (TL1, and TL2) under an effective normal stress of 75 kPa contributed to shear strength of T by 19 and 24%, respectively. Similarly, TB1 and TB2 have higher shear strength values (76 and 88 kPa, respectively), compared with that of T (63 kPa). It can be concluded that the compost treatment increases the shear strength, particularly under high normal stresses, due to their relatively higher friction angles of pure compost as compared to topsoil.

Le et al. (2015) compared the shear stress values of 20% compost (nutrient rich compost consists of yard trimmings) amended high plasticity clay soil under varying effective normal stresses. The results yielded that the compost treatment showed no increase under effective normal stresses of 50 and 100 kPa, whereas 25% and 23% increases were observed under effective normal stresses of 200 and 400 kPa, respectively.

Results of the slope stability analyses are summarized in Table 3. Figure 8 represents an example output; analysis of 5-cm uppermost topsoil layer for a 7-m height and 2:1 steep slope under saturated conditions, where the factor of safety is 2.422. Analyses show that slopes that consist of higher compost have higher factors of safety (FS) under unsaturated conditions and lower FS under saturated conditions, compared

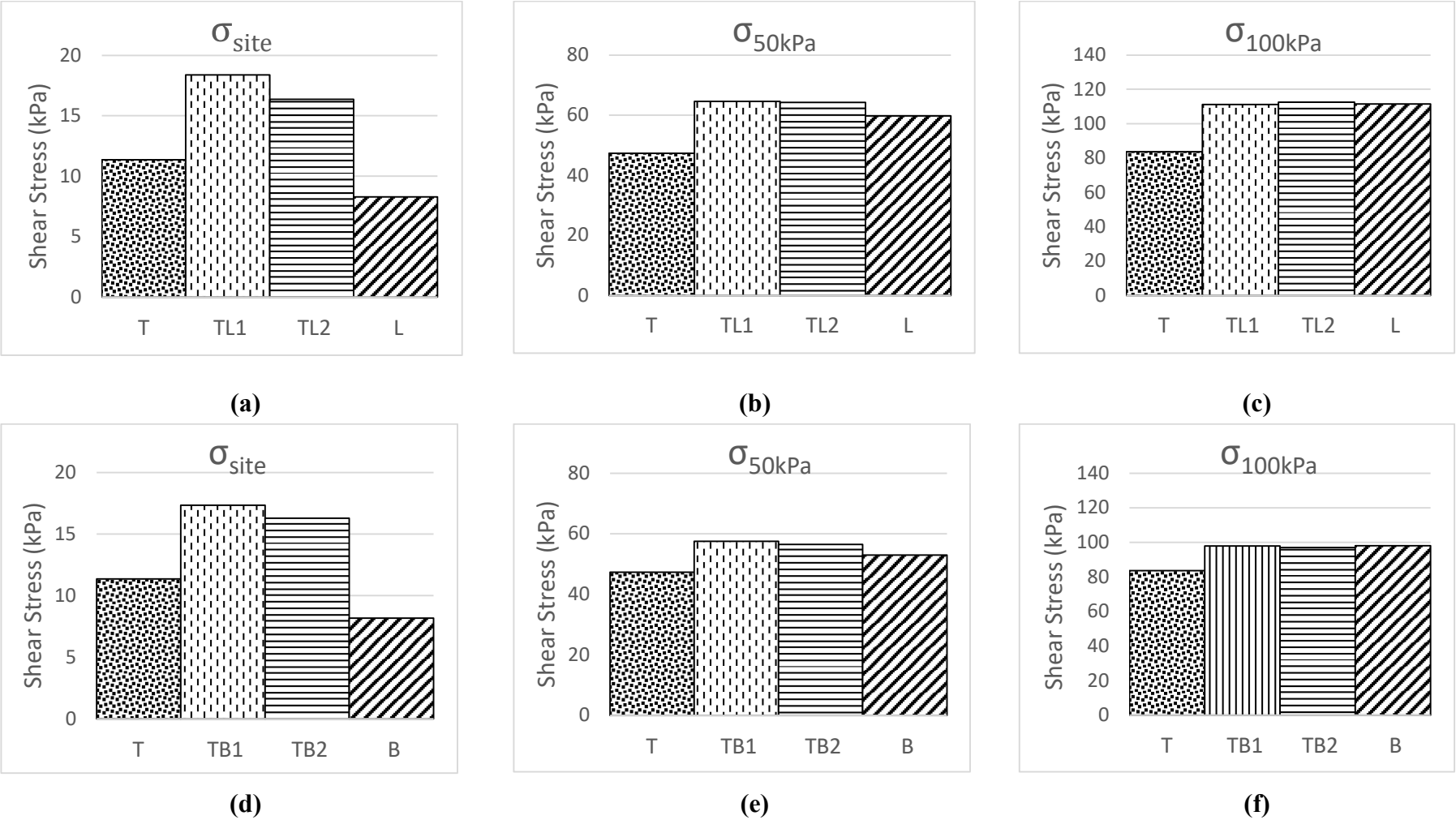

Figure 6. Direct shear results under the effective normal stresses of site condition (0.2 to 0.5 kPa) (a and d), 50 kPa (b and e), and 100 kPa (c and f) by leaf compost and biosolids amendment

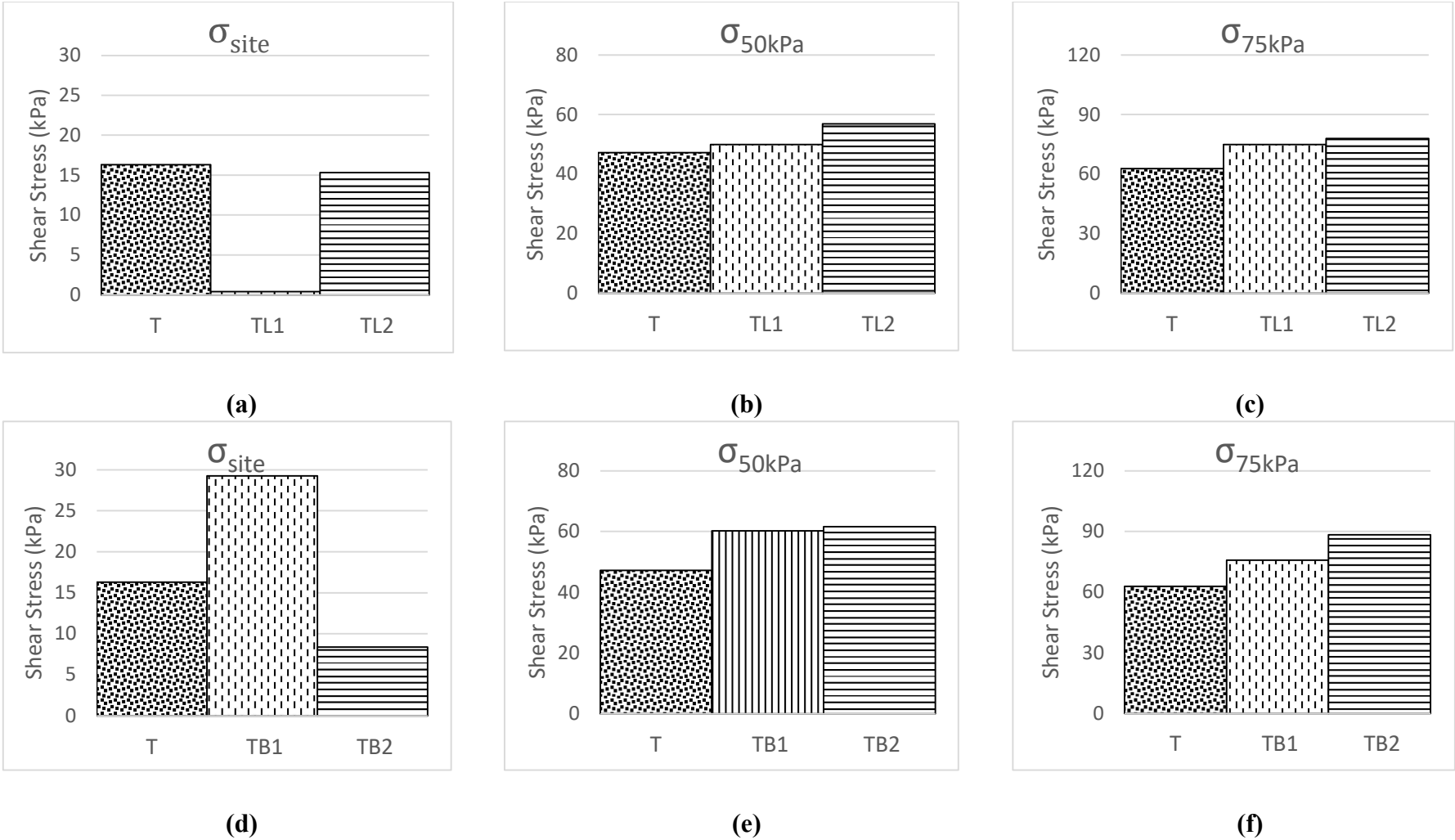

Figure 7. CU triaxial results under the effective normal stresses of site condition (0.2 to 0.5 kPa) (a and d), 50 kPa (b and e), and 75 kPa (c and f) by leaf compost and biosolids amendment

Table 3. Results of slope stability analyses

Material	FS Based on Parameters Derived from the Direct Shear Tests				FS Based on Parameters Derived from the CU Triaxial Tests			
	7 m - height		12 m - height		7 m - height		12 m - height	
	Saturated	Unsaturated	Saturated	Unsaturated	Saturated	Unsaturated	Saturated	Unsaturated
T	2.422	3.535	1.732	2.731	2.425	3.540	1.733	2.732
B	2.420	3.544	1.729	2.737	NA	NA	NA	NA
L	2.420	3.542	1.730	2.735	NA	NA	NA	NA
TB1	2.423	3.541	1.732	2.733	2.431	3.549	1.735	2.736
TB2	2.424	3.544	1.732	2.735	2.420	3.540	1.731	2.733
TL1	2.426	3.544	1.733	2.734	2.417	3.527	1.729	2.727
TL2	2.424	3.544	1.732	2.735	2.424	3.543	1.732	2.734

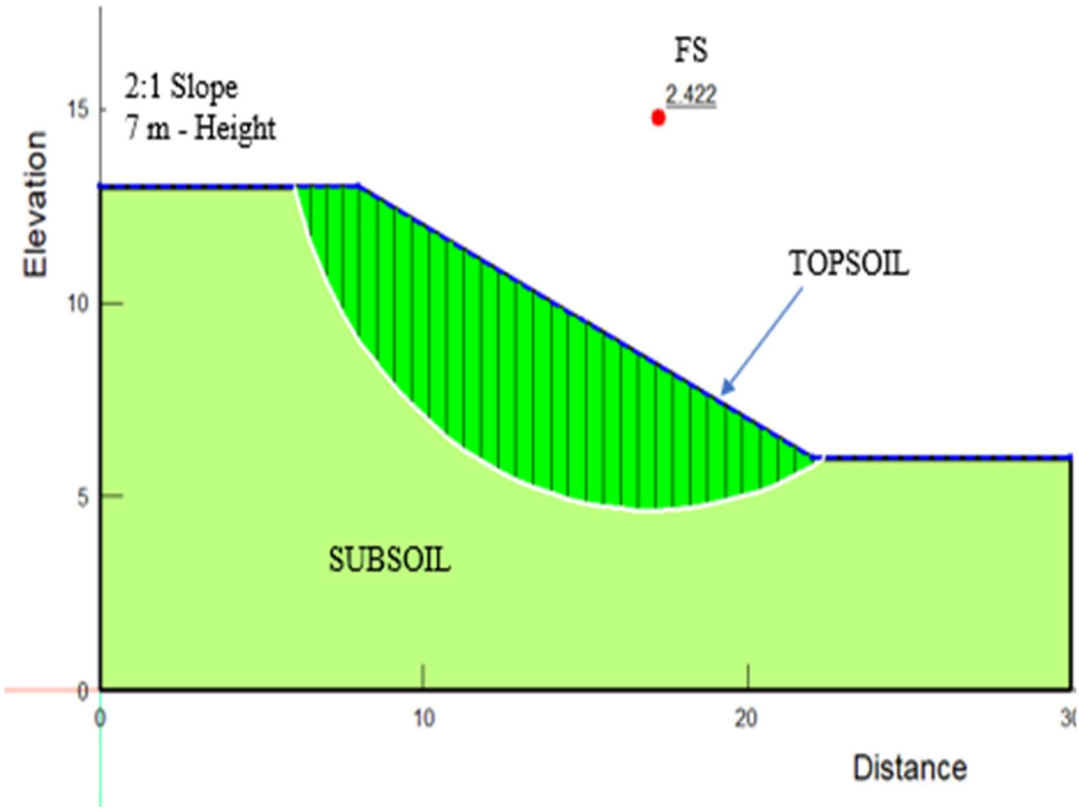

Figure 8. Example slope stability analysis of topsoil using direct shear test parameters under saturated conditions

with T, associated with higher effective friction angles of the composts. 7-m height slope has FS=2.417-2.431 for saturated, and FS=3.527-3.549 for unsaturated conditions. 12-m height slope has relatively lower FS as expected, 1.729-1.735 for saturated, and 2.727-2.737 for unsaturated conditions. Comparisons between factors of safety calculated by direct shear parameters and CU triaxial test parameters are modest, with a maximum difference of ± 0.017. Overall, effect of compost treatment on FS is very little, under any given condition.

Shape parameters of topsoil, composts, and compost amended topsoils are summarized in Table 4. All materials have moderate angularities, and the angularity increases by compost amendment. T has the lowest angularity of 2607.5 ± 1390.6, where B and L have the highest angularities of 3197.1 ± 1398.9 and 3329.1 ± 1394.5, respectively. Form 2D is defined by Equation 4 and applies to particle sizes smaller than 4.75 mm. It has a range of 0 to 20, where a perfect circle has a value of zero. Form 2D results show that T has the lowest Form 2D (i.e., has the most circular particles) of 7.53 ± 3.00, whereas B and L have the Form 2D values of 9.45 ± 3.69 and 9.03 ± 3.32, respectively. Texture, elongation, sphericity, and flatness parameters were obtained for particles greater than 4.75-mm per AIMS guidelines. Texture values indicate that the particles of T have the smoothest surface (i.e., the lowest texture value) with a value of 249.5 ± 215.6, and B and L have the highest texture values of 515.5 ± 149.2 and 494.5 ± 160.1, respectively. Results also indicate that T has relatively less flat and elongated particles, compared to those of composts. Both flatness and elongation have a scale of 0 to 1, where zero indicates the flattest and the most elongated particle shape. B and L have the elongation ratios of 0.51 ± 0.18 and 0.66 ± 0.23, respectively, whereas the

Table 4. Summary of the shape property results

Material	Shape Properties					
	Angularity	**Form 2D**	**Texture**	**Elongation**	**Sphericity**	**Flatness**
T	2607.5 ± 1390.6	7.53 ± 3.00	249.5 ± 215.6	0.72 ± 0.19	0.75 ± 0.14	0.88 ± 0.11
B	3197.1 ± 1398.9	9.45 ± 3.69	515.5 ± 149.2	0.51 ± 0.18	0.59 ± 0.14	0.82 ± 0.13
L	3329.1 ± 1394.5	9.03 ± 3.32	494.5 ± 160.1	0.66 ± 0.23	0.69 ± 0.18	0.80 ± 0.13
TB1	2973.3 ± 1385.4	8.82 ± 3.58	416.2 ± 242.1	0.67 ± 0.19	0.71 ± 0.14	0.82 ± 0.11
TB2	3106.5 ± 1429.9	9.45 ± 3.91	489.1 ± 226.2	0.55 ± 0.20	0.61 ± 0.14	0.78 ± 0.10
TL1	2895.6 ± 1402.6	8.41 ± 3.36	315.7 ± 200.3	0.73 ± 0.17	0.76 ± 0.13	0.84 ± 0.12
TL2	3127.0 ± 1461.4	8.37 ± 3.18	319.5 ± 220.5	0.70 ± 0.19	0.74 ± 0.14	0.85 ± 0.10

elongation ratio of T is 0.72 ± 0.19. B and L also show relatively lower sphericities of 0.59 ± 0.14 and 0.69 ± 0.18, respectively, and T has a sphericity of 0.75 ± 0.14.

A parametric study was conducted to relate the shape parameters to shear parameters of topsoil, composts, and compost amended topsoils. Angularity and Form 2D were the parameters that provided the best relationship for B and L treated topsoils, with an R^2 of 0.898 and 0.891 for the angularity, and an R^2 of 0.800 and 0.938 for the Form 2D, respectively (Figure 9). The data in Figure 9 reveals that the friction angle increases with an increase in angularity, and particles having relatively less circular shape (i.e., more elongated shape) exhibited higher friction angle. Previous studies also report an increase in friction angle with an increase in angularity (Koerner, 1970; Shinohara et al., 2000; Cho et al. 2006; Li, 2013). The remaining shape parameters, which were obtained for particles greater than 4.75 mm, yielded an R^2 of less than 0.7 (ranging from 0.39 to 0.86) and all correlations are presented in Figures C4 and C5 of Appendix C. In addition to use of limited types of compost and topsoil, particle selection (e.g., selecting particles with a size greater than 4.75 mm) solely based on size can be another reason for obtaining low R^2 values during the image analysis. Figure C6 in Appendix C, for instance, shows two different leaf compost particles having the same particle size range (>4.75 mm) with entirely different shape characteristics.

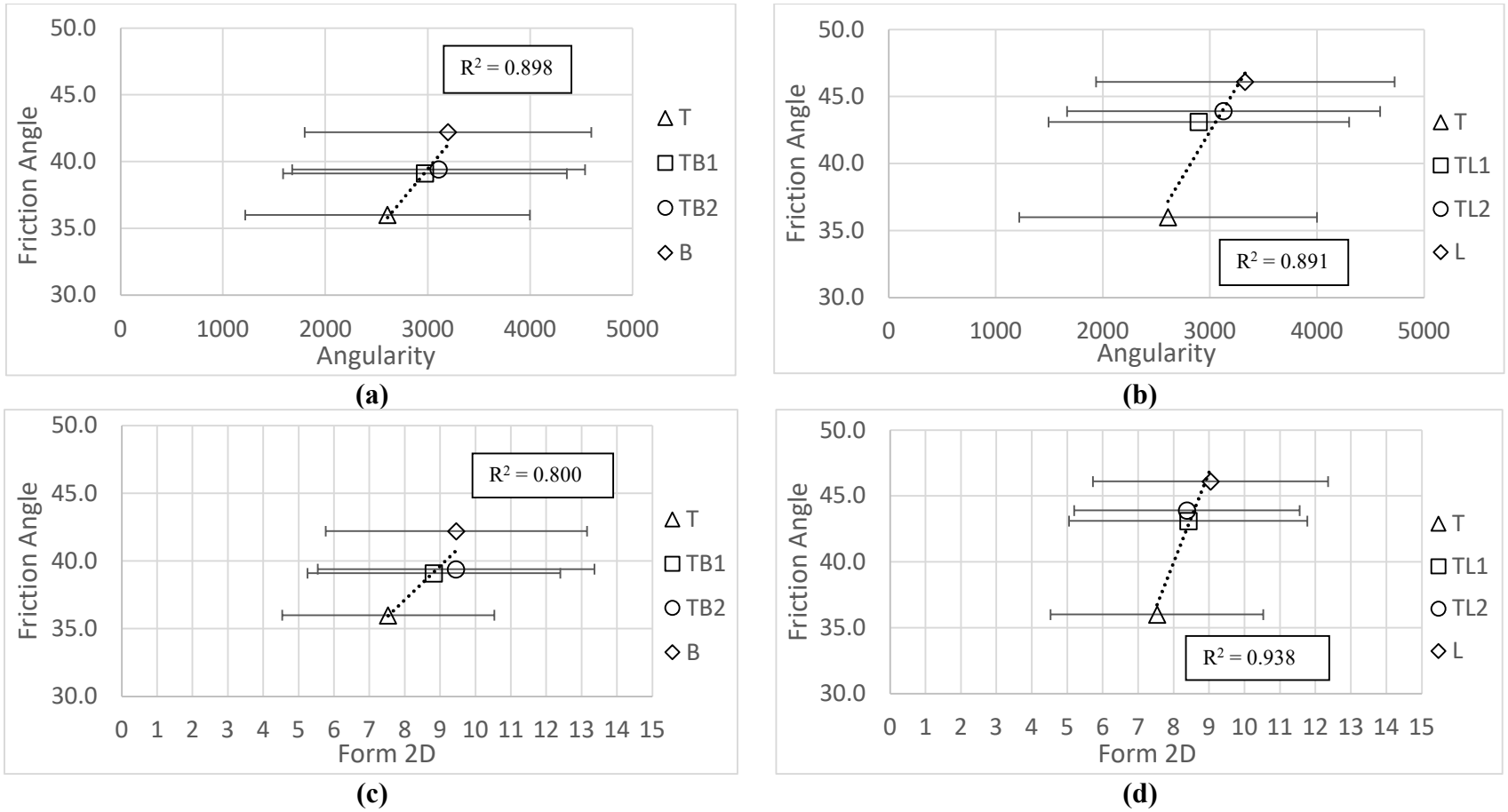

Figure 9. Correlation between angularity and friction angle by (a) B and (b) L amendment, and between the Form 2D and friction angle by (c) B and (d) L amendment

3.2 Results of Hydraulic Tests

3.2.1 Results of Saturated Hydraulic Conductivity Tests

Saturated hydraulic conductivities of the materials at their optimum, $K_{s,opt}$, and at +5% wet of optimum water contents ($K_{s,opt+5}$) are summarized in Table 5. Temporal characteristics of the hydraulic conductivities are given in Figure 10. Results indicate that T has the lowest hydraulic conductivity, 1.2 x 10^{-7} cm/s, whereas the highest hydraulic conductivities are measured for the two composts B and L (7.4 x 10^{-4} and 1.3 x 10^{-4} cm/s, respectively). $K_{s,opt}$ of the blends remain between those of T and the two composts, and varies between 1.7 x 10^{-6} and 5.5 x 10^{-6} cm/s. $K_{s,opt}/K_{s,opt+5}$ ratios were calculated to analyze the effect of water content on saturated hydraulic conductivity (Table 5). Each material exhibits a relatively lower $K_{s,opt+5}$, compared to its corresponding $K_{s,opt}$, and the $K_{s,opt}/K_{s,opt+5}$ ratios vary from 1.3 (L) to 4.0 (TB1). Observing lower hydraulic conductivities at wet of optimum was consistent with the study of Puppala et al. (2004), where 5% increase in water content decreased the hydraulic conductivities of biosolids and dairy manure compost amended clayey soils by approximately 2 to 10 times.

Changes in hydraulic conductivity by compost, gravel, sand, and fines contents, and characteristic particle sizes (i.e., D_{10}, D_{30}, D_{50}, and D_{60}) are presented in Figures 11-13. Due to compost addition, $K_{s,opt}$ of topsoil increases with increasing grain size, which was expected as the particle size is one of the main properties that influences hydraulic conductivity (Hubbert, 1940; Olanrewaju and Wong, 1994; Puppala et al., 2004).

Table 5. Summary of the saturated hydraulic conductivity test results

Material	K_s (cm/s)		$K_{s,opt}/K_{s,opt+5}$
	w_{opt} (%)	w_{opt+5} (%)	
T	1.2×10^{-7}	3.7×10^{-8}	3.4
B	7.4×10^{-4}	4×10^{-4}	1.8
L	1.3×10^{-4}	9.8×10^{-5}	1.3
TB1	2×10^{-6}	4.9×10^{-7}	4.0
TB2	5.5×10^{-6}	3.5×10^{-6}	1.6
TL1	1.7×10^{-6}	6.1×10^{-7}	2.8
TL2	3.6×10^{-6}	2.4×10^{-6}	1.5

Notes: K_s: saturated hydraulic conductivity at w_{opt}, $K_{s,opt+5}$: saturated hydraulic conductivity at w_{opt+5}, w_{opt}: optimum water content, w_{opt+5}: +5% of optimum water content

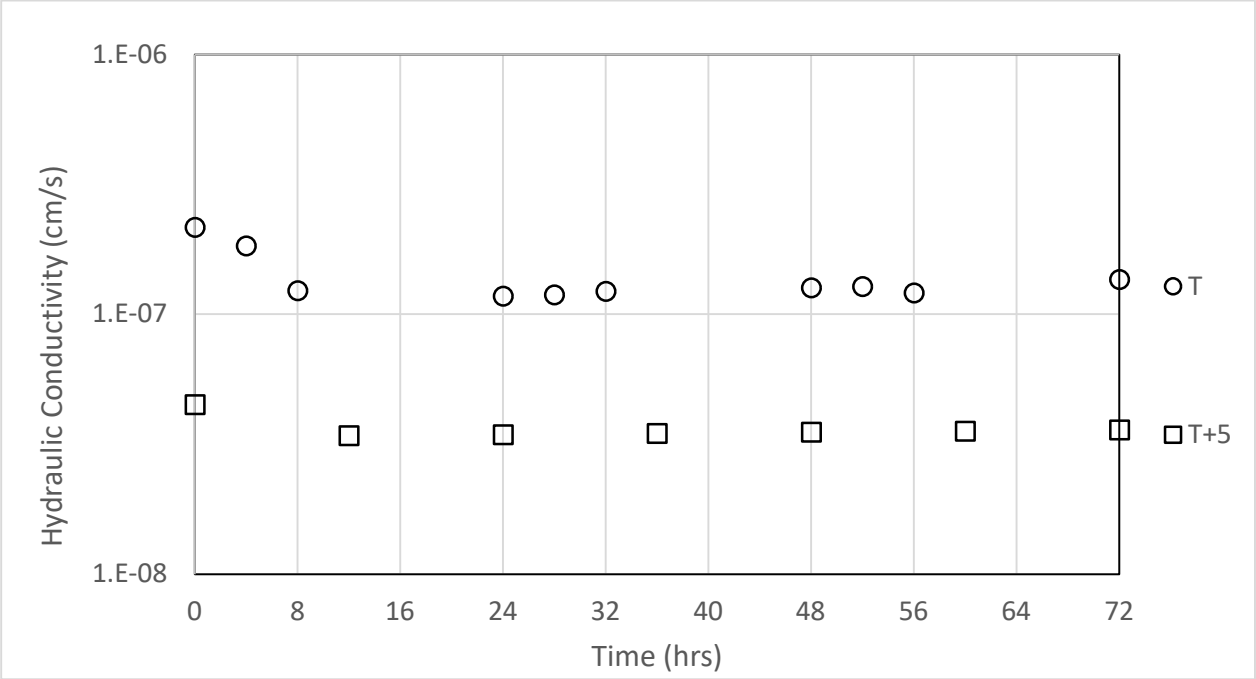

(a)

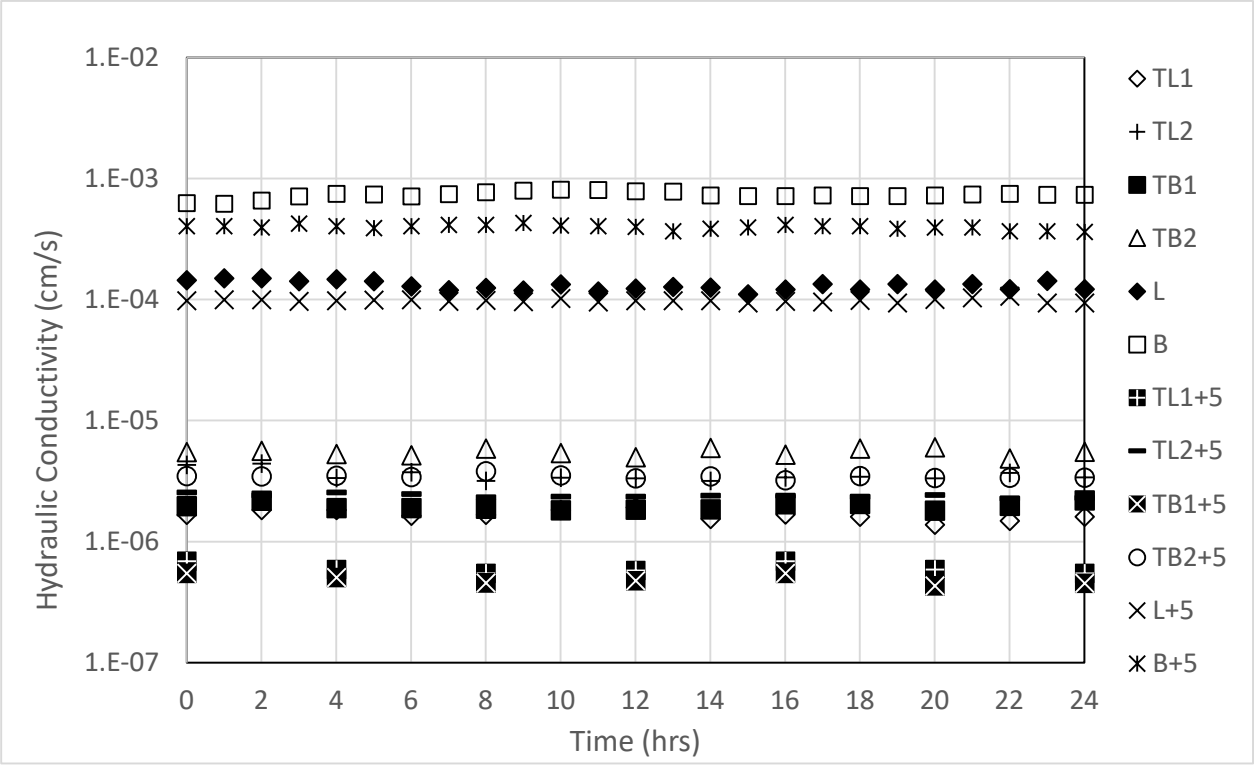

(b)

Figure 10. Saturated hydraulic conductivity of (a) topsoil (b) composts and compost-amended topsoils, at w_{opt} and w_{opt+5}

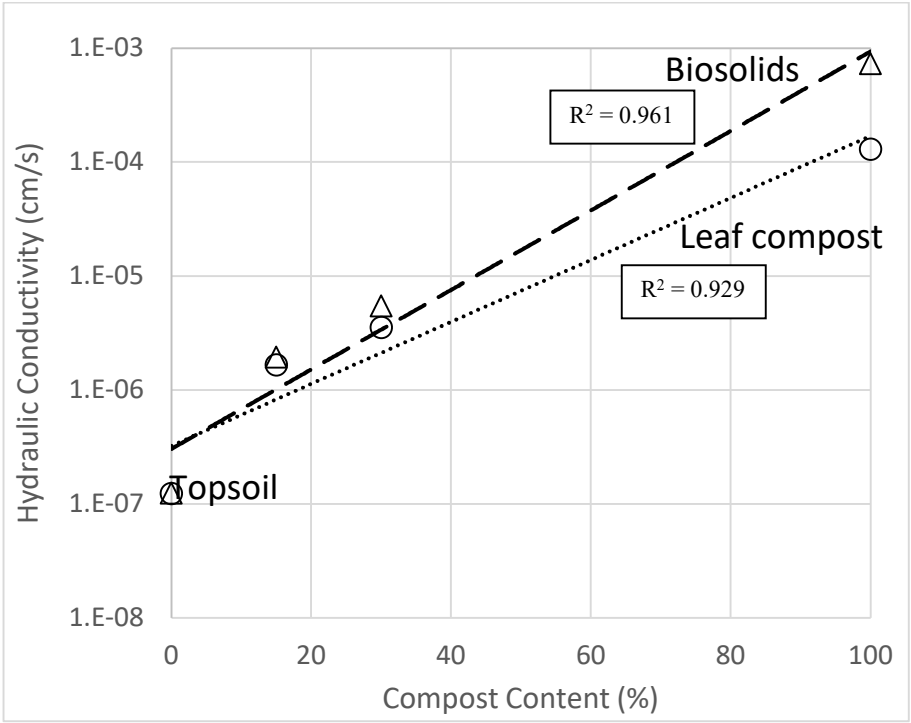

(a)

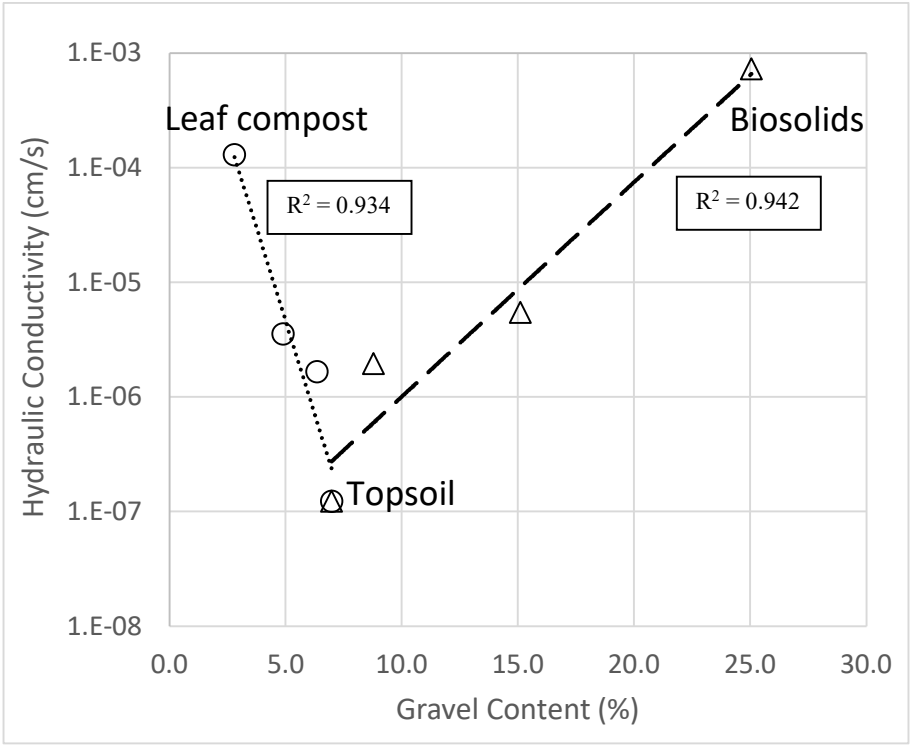

(b)

Figure 11. Effect of (a) compost and (b) gravel content on saturated hydraulic conductivity of topsoil, composts, and compost-amended topsoils

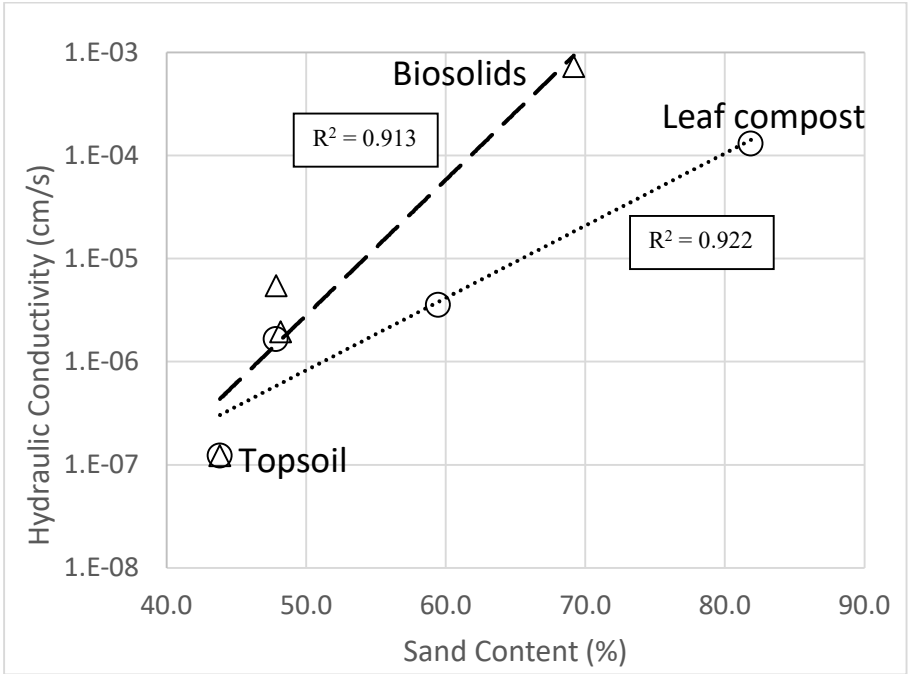

(a)

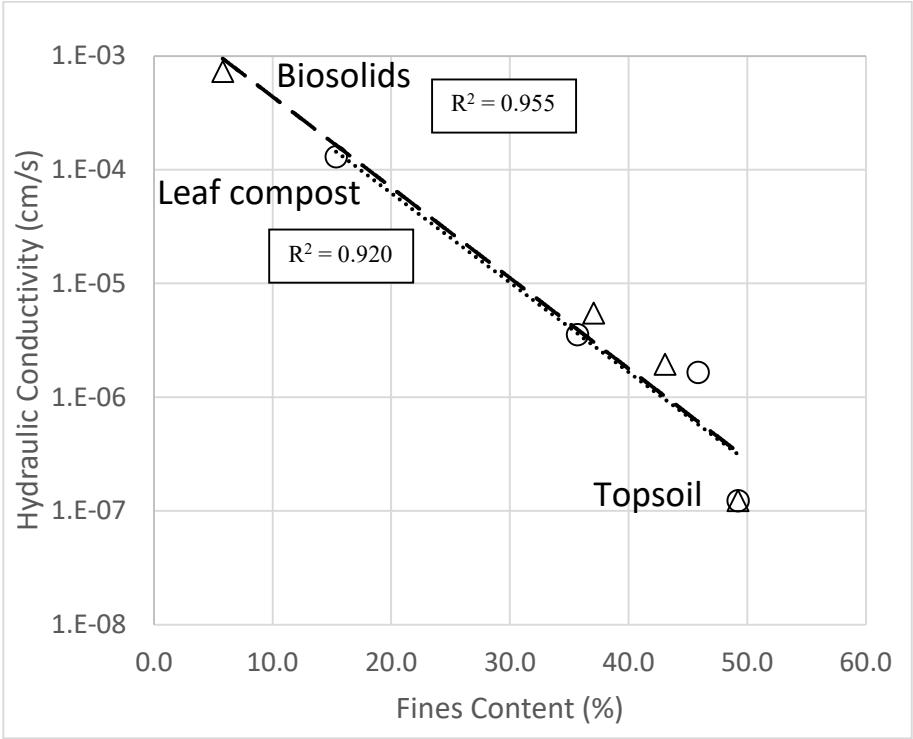

(b)

Figure 12. Effect of (a) sand and (b) fines content on saturated hydraulic conductivity of topsoil, composts, and compost-amended topsoils

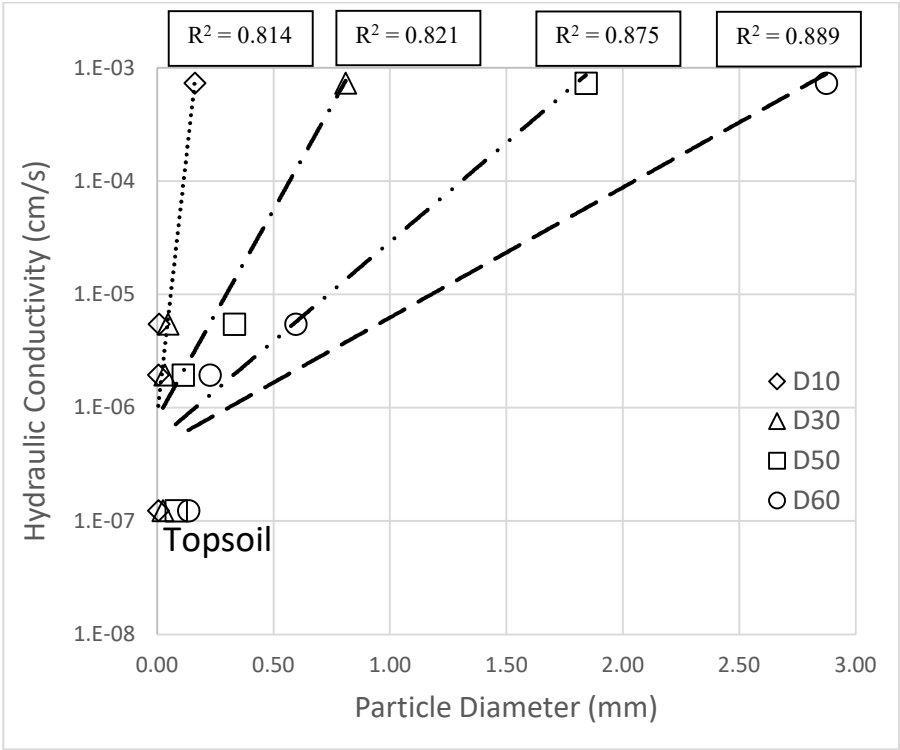

(a)

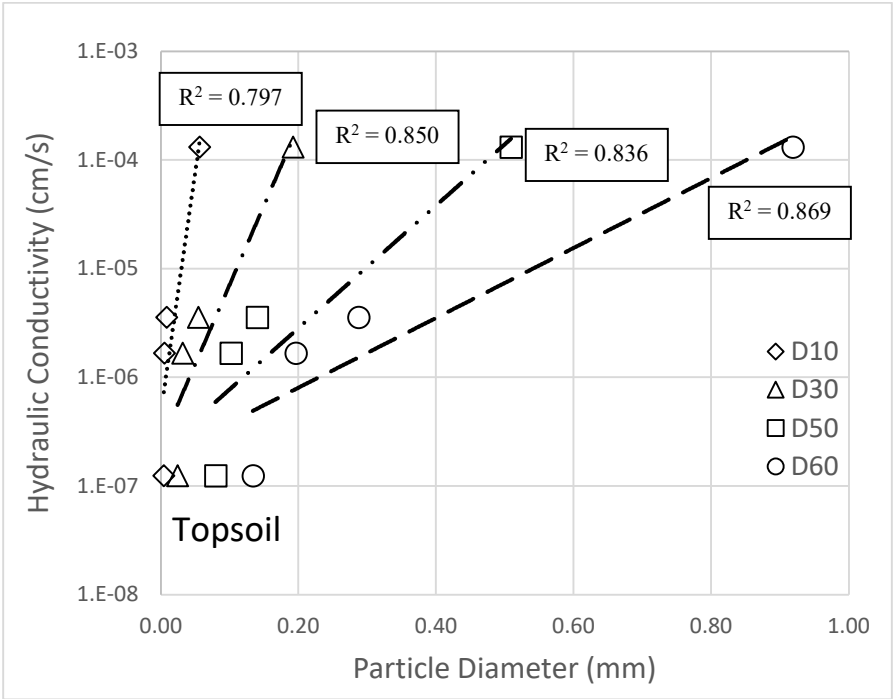

(b)

Figure 13. Effect of grain size on hydraulic conductivity by (a) biosolids and (b) leaf compost amendment

Biosolids compost (B) amendment increases the hydraulic conductivity of T by 16 - 6000 times accompanied with a decrease in fines content from 49.2% to 5.8%, an increase in sand content from 43.8 to 69.1%, and an increase in gravel content from 7 to 25.1% (Figures 11 and 12). Effect of L addition to topsoil on hydraulic conductivity is less pronounced, and the hydraulic conductivity increases 13 - 1000 times coupled with a decrease in fines content from 49.2 to 15.3%, an increase in sand content from 43.8 to 81.9%, and a decrease in gravel content from 7 to 2.8%. Higher increases in hydraulic conductivity due to B amendment can be attributed to the higher gravel content (25.1% versus 2.8%) and lower fines content (5.8% versus 15.3%) of this compost.

Figure 13 shows that the hydraulic conductivities of the materials increase with increasing characteristic grain sizes of the soil (i.e., D_{10}, D_{30}, D_{50}, and D_{60}). The hydraulic conductivity seems to be more sensitive to smaller grain sizes (D_{10} and D_{30}) when compared to larger sizes (D_{50} and D_{60}), consistent with the previous studies that finer sizes play a major role on hydraulic conductivity (FHWA, 2004; Siahdashti et al. 2015; Hatipoglu et al., 2020). An increase in D_{10} yielded the highest rate of increase in hydraulic conductivity of compost-amended topsoils. It is believed that fines contents of all the materials tested, which ultimately affect D_{30} and D_{10}, have a direct influence on changes in hydraulic conductivity.

3.2.2 Results of Unsaturated Hydraulic Tests

Soil-water characteristics and fitting parameters of van Genuchten constrained (1980) and van Genuchten/Mualem models were obtained using HYPROP Measurement

System (HMS). Equations (1) and (2) are used to develop the soil-water characteristics and unsaturated hydraulic conductivity versus volumetric water content curves in Figures 14 and 15, respectively. During the development of soil-water characteristic curves, K_s (saturated hydraulic conductivity) can be estimated as the hydraulic conductivity at saturated volumetric water content. Alternatively, laboratory-measured saturated hydraulic conductivity values per ASTM D5084 can be input into the HMS before using the van Genuchten/Mualem models.

Tables 6 and 7 summarize the model parameters and the root mean squares errors (RMSE) for the two approaches. The RMSE stands for the average difference between the measured volumetric water content and the fitted curve (Pertassek et al., 2011). For instance, T has an RMSE of 0.0013, which states that the average difference between the volumetric water content of data points and fitted curve is 0.13%. Models without any predefined (lab-measured) values of K_s yielded relatively lower RMSE values. Better fits (lower RMSE values) were observed for the soil-water characteristic (i.e., retention) curves as compared to unsaturated hydraulic conductivity-volumetric water content curves in both cases.

Estimated K_s of T and B are 26 and 11 times higher, respectively, than those measured using the ASTM D5084 procedure, while the estimated and measured K_s values are comparable for the remaining materials. Topsoil, composts, and the blends tested in the current study are coarse-textured materials. Bezerra-Coelho et al. (2017) indicated that K_s and tortuosity (τ) can be predicted by the van Genuchten/Mualem model more accurately for fine and medium-textured soils as compared to coarse and very coarse-textured soils. It should also be noted that the unsaturated hydraulic

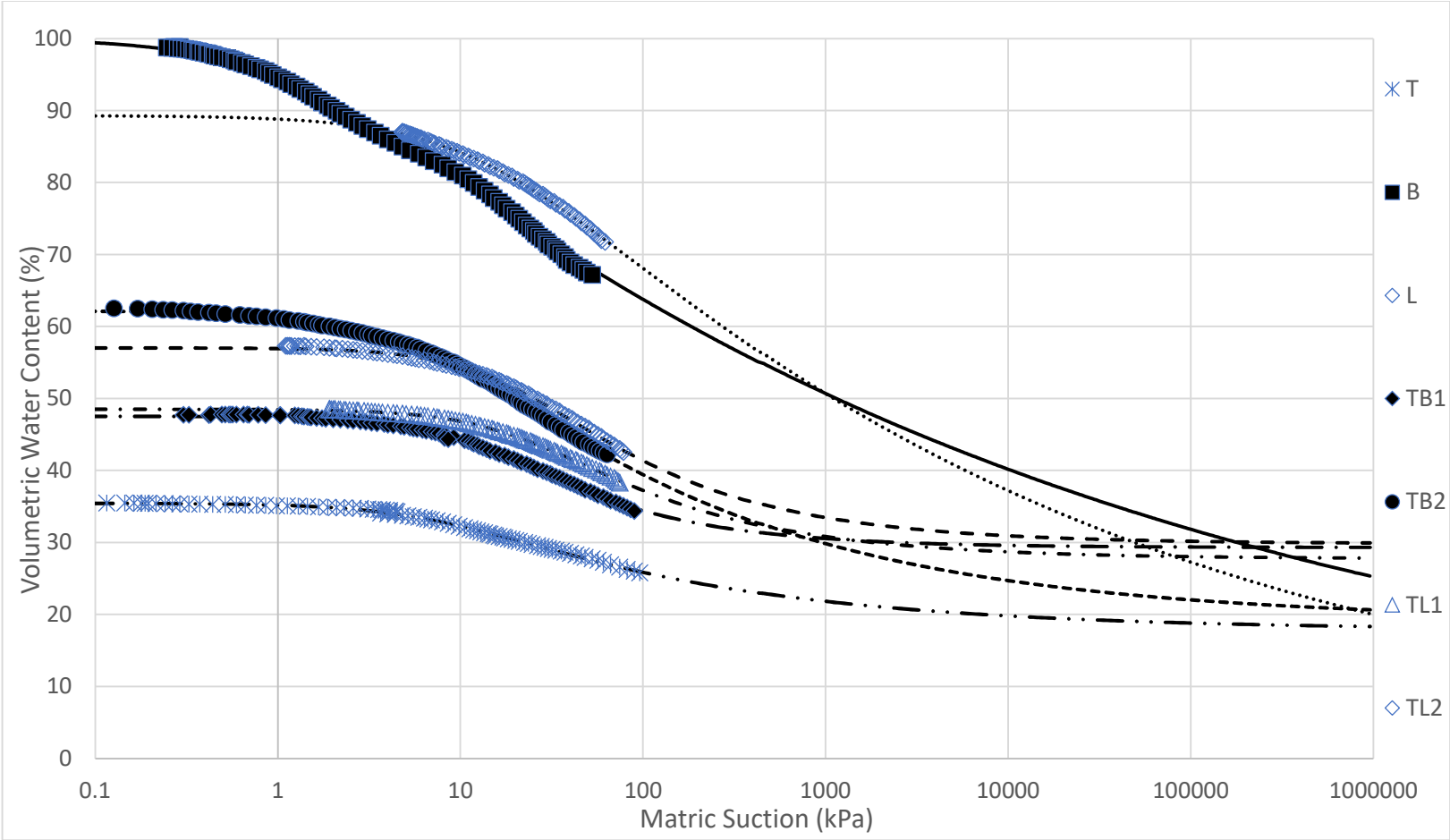

Figure 14. Soil-water characteristic curves of the materials tested (lines indicate fits by the van Genuchten (1980) model)

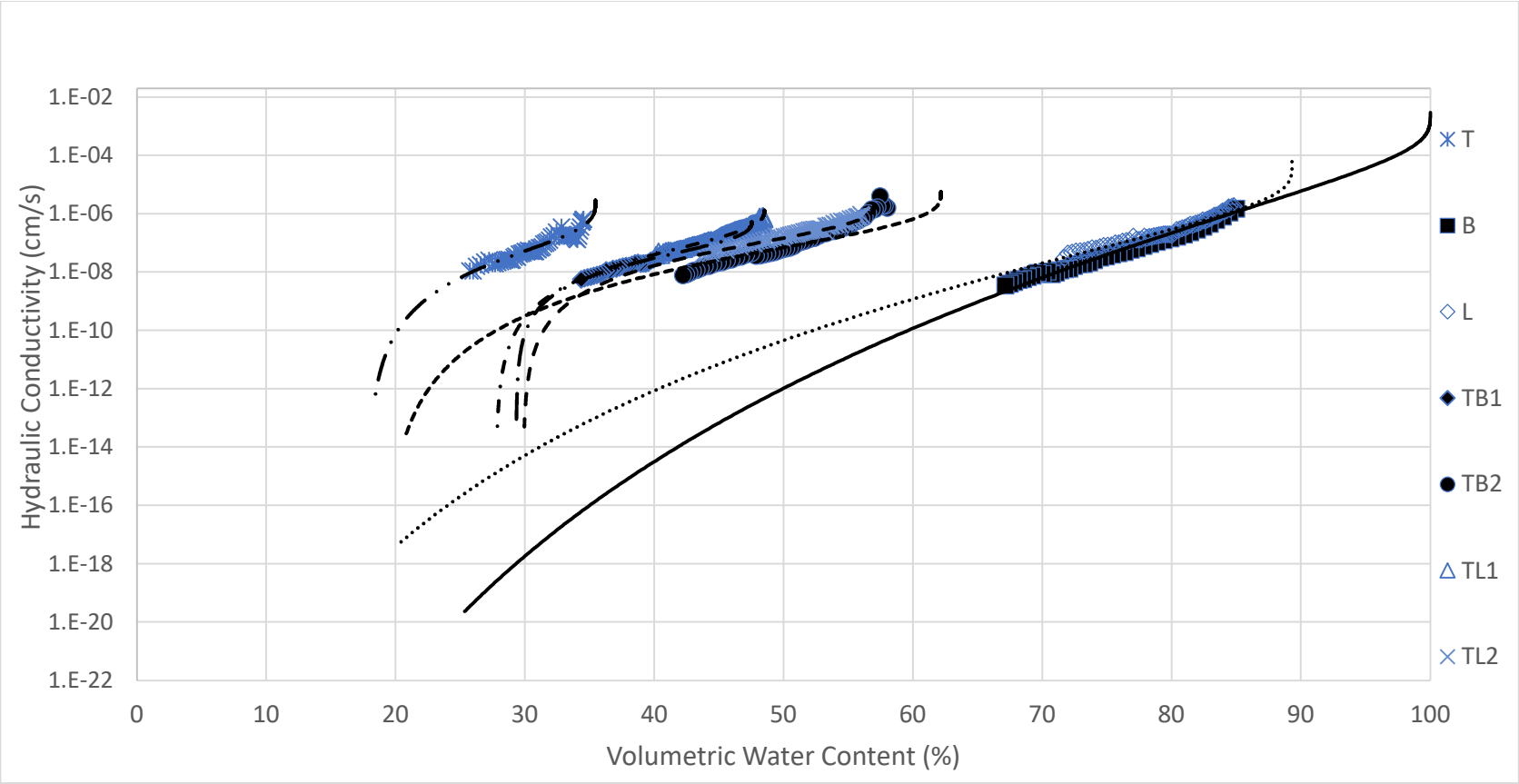

Figure 15. Hydraulic conductivity versus volumetric water content of the materials tested (lines indicate fits by the van Genuchten/Mualem model)

Table 6. Model parameters and RMSEs for van Genuchten constrained (1980) and van Genuchten /Mualem models by estimated K_s

Material	θ_s (%)	θ_r (%)	n (-)	α (cm^{-1})	$K_{s\ estimated}$ (cm/s)	τ (-)	RMSE (Ks estimated)	RMSE (θ)
T	35.5	17.9	1.310	0.0118	3.1×10^{-6}	-4.804	0.1431	0.0013
B	100	0	1.101	0.0821	7.9×10^{-3}	4.082	0.0398	0.0062
L	89.3	0	1.134	0.0065	9.6×10^{-5}	0.874	0.0707	0.0017
TB1	47.5	29.3	1.625	0.0071	5.3×10^{-7}	-3.096	0.1160	0.0023
TB2	62.2	19.1	1.283	0.0133	6.2×10^{-6}	-4.079	0.2652	0.0037
TL1	48.5	27.8	1.508	0.0042	1.3×10^{-6}	-3.086	0.0621	0.0007
TL2	57.0	29.8	1.519	0.0047	2.1×10^{6}	-3.100	0.1464	0.0021

Notes: θ_s: saturated volumetric water content, θ_r: residual water content, n: shape parameter related to bending of the retention curve, α: shape parameter [cm^{-1}] linked with the inverse of the air-entry pressure, $K_{s\ estimated}$: saturated hydraulic conductivity estimated, τ: tortuosity parameter, $RMSE_{(Ks\ estimated)}$: root mean squares error of van Genuchten/Mualem model, $RMSE_{(\theta)}$: root mean squares error of van Genuchten (1980) model

Table 7. Model parameters and RMSEs for van Genuchten constrained (1980) and van Genuchten /Mualem models using K_s measured by ASTM D5084 procedure

Material	θ_s (%)	θ_r (%)	n (-)	α (cm^{-1})	K_s (cm/s)	τ (-)	RMSE (Ks)	RMSE (θ)
T	35.0	26.9	2.806	0.0076	1.2×10^{-7}	-2.786	0.2936	0.0057
B	99.5	25.7	1.153	0.0664	7.4×10^{-4}	-0.664	0.1188	0.0070
L	91.8	0	1.125	0.0071	1.3×10^{-4}	1.135	0.0760	0.0014
TB1	47.8	10.4	1.228	0.0072	2×10^{-6}	-5.718	0.1543	0.0012
TB2	62.1	21.8	1.309	0.0131	5.5×10^{-6}	-3.821	0.2602	0.0039
TL1	48.6	24.4	1.422	0.0040	1.7×10^{-6}	-3.344	0.0642	0.0005
TL2	57.2	17.9	1.329	0.0045	3.6×10^{-6}	-3.928	0.1602	0.0013

Notes: θ_s: saturated volumetric water content, θ_r: residual water content, n: shape parameter related to bending of the retention curve, α: shape parameter [cm^{-1}] linked with the inverse of the air-entry pressure, K_s: saturated hydraulic conductivity measured in the laboratory, τ: tortuosity parameter, $RMSE_{(Ks)}$: root mean squares error of van Genuchten/Mualem model, $RMSE_{(\theta)}$: root mean squares error of van Genuchten (1980) model

conductivity is strongly affected by anisotropy throughout the drying process (Zhang et al., 2003), which may have caused the difference between the estimated and measured K_s in the current study.

Field capacity (FC), wilting point (WP), and available water content (AWC) are defined in Figure 3, and these parameters measured in the current study without any predefined values of K_s are listed in Table 8. Organic matter (OM) is one of the significant parameters that affects the plant available water content (AWC) (Zibilske et al., 2000; Zare et al., 2010; Siahdashti et al., 2015). Minasny and McBratney (2018) stated that 1% organic carbon addition by weight could result in an average of 1.16% increase on the volumetric water content. Maynard and Hill (1994) stated that leaf compost that has a 75-mm layer thickness raised the AWC by approximately 2.5 times compared to a sandy soil and presented nearly a 7-day available water for plants.

The data in Table 8 shows that there is an increase in the available water content by compost treatment. T has an AWC of 10.9%, while B and L have higher AWC values of 31.6 and 36.4%, respectively, and those of blends vary between T and composts. Compost amendment increases the AWC of T by approximately 1.4-2.6 times, which can lead to an improvement in plant growth establishment and erosion control (Gonzalez and Cooperband, 2002; Jennings et al., 2003; Kirchoff et al., 2003; Veeresh et al., 2003).

Contrary to common observations for saturated hydraulic conductivity, unsaturated hydraulic conductivity (hydraulic conductivity at $\theta<100\%$) decreases with an increase in pore size due to a faster drying process in larger pores, mainly when soil exerts high matric potential (Al-Riffai, 2005). Moreover, capillary pore filling

Table 8. AWC, FC, WP and corresponding hydraulic conductivities.

	K_{FC} (cm/s)	K_{WP} (cm/s)	FC (%)	WP (%)	AWC (%)
T	1.3×10^{-7}	4.4×10^{-10}	32.3	21.4	10.9
B	2.2×10^{-7}	4.4×10^{-13}	80.2	48.6	31.6
L	1×10^{-6}	1.9×10^{-11}	84.3	47.9	36.4
TB1	9.2×10^{-8}	1.5×10^{-10}	44.5	30.3	14.2
TB2	1.6×10^{-7}	1.5×10^{-10}	54.4	28.7	25.7
TL1	2.8×10^{-7}	3.3×10^{-10}	46.9	30.2	16.7
TL2	4×10^{-7}	4.8×10^{-10}	54.5	32.8	21.7

Notes: K_{FC}: hydraulic conductivity at field capacity, K_{WP}: hydraulic conductivity at wilting point, FC: field capacity, WP: wilting point, AWC: available water content.

plays a major role in hydraulic conductivity, especially at matric suctions greater than the suction that corresponds to the field capacity (i.e., 10-30 kPa). As water drainage occurs, water films are generated in between soil particles and flow path along water films becomes more tortuous (i.e., longer), resulting in a decrease in observed hydraulic conductivity. Tokunaga (2009) showed that the soils with higher fines contents have higher unsaturated hydraulic conductivities compared to those with coarser size particles under high matric potential, due to existence of greater water film perimeter length per cross-sectional area in soil having finer-size particles. Shinomiya et al. (2000) and Vereecken et al. (2010) also showed that the decrease in unsaturated hydraulic conductivity becomes sharper with an increase in tortuosity.

The data in Table 8 and Figure 16 show that the unsaturated hydraulic conductivity decreases by 2 to 6 orders of magnitude from the field capacity (K_{FC}) to the wilting point (K_{WP}). Biosolids and leaf compost exhibited the greatest decreases from K_{FC} to K_{WP}, and they have the lowest K_{WP} of 4.4×10^{-13} and 1.9×10^{-11} cm/s, respectively, most probably associated with their pore size distributions as well as the tortuosities. K_{WP} of topsoil (4.4×10^{-10} cm/s) and blends ($1.5\text{-}4.8 \times 10^{-10}$ cm/s) are comparable. Rate of decreases from K_{FC} to K_{WP} for the blends remain between those of topsoil and composts. No clear-cut trend can be observed between the rate of decrease and compost content.

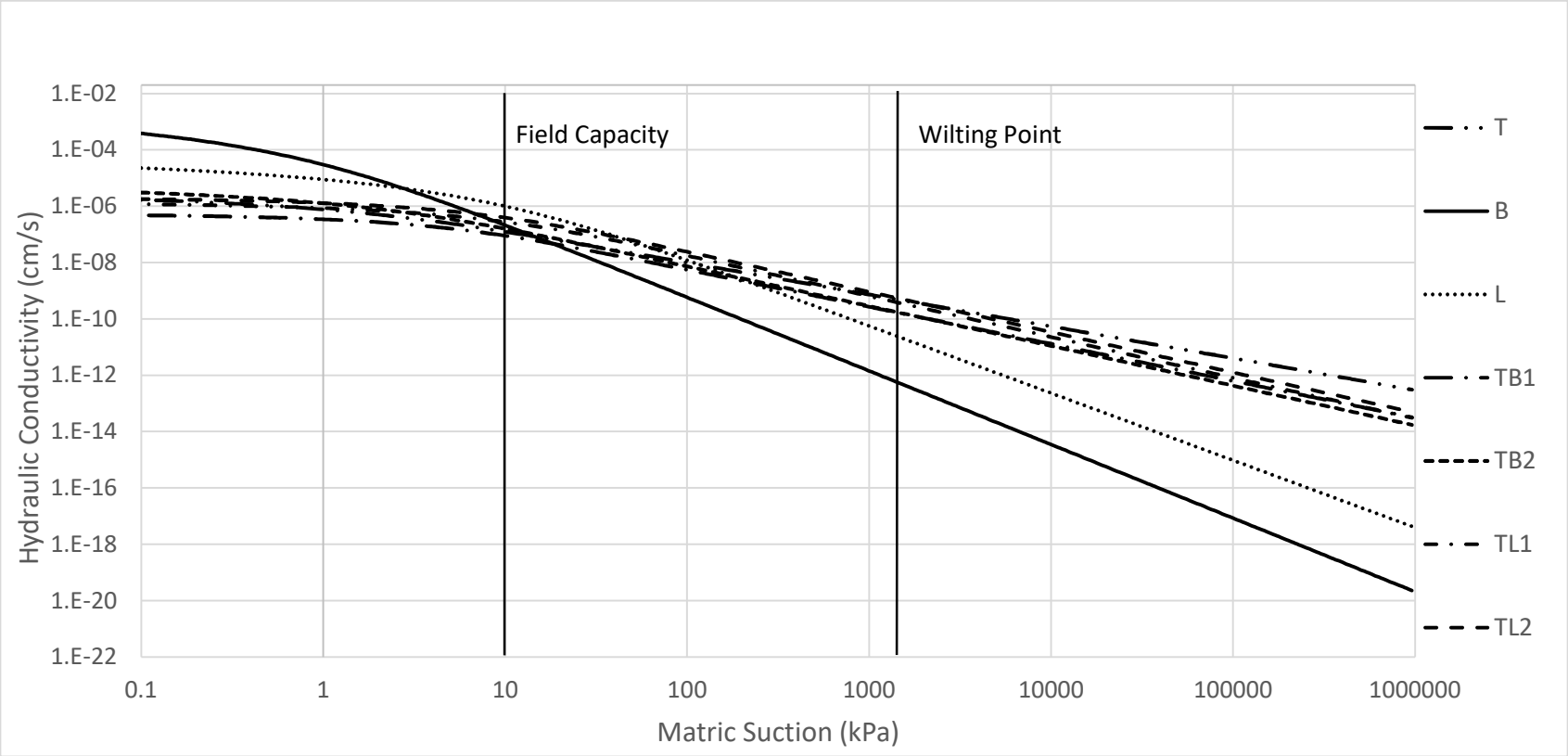

Figure 16. Hydraulic conductivity versus matric suction of the materials tested

Chapter 4

Conclusions

4.1 Summary and Conclusions

A research study was undertaken to define geotechnical properties of two composts (biosolids and leaf compost) and compost-amended topsoils for their possible use on highway slopes. Direct shear and consolidated-undrained (CU) triaxial compression tests were performed to investigate the shear strength properties of the materials. Stabilities of 7-12 m high slopes were analyzed by using the obtained shear strength parameters. Digital image analyses were performed to determine shape parameters and their relationship to measured internal friction angles. Flexible-wall hydraulic conductivity tests and HYPROP measurement system were used to define the saturated and unsaturated hydraulic properties of each material. The following conclusions were warranted:

1) Effective friction angle of topsoil measured in direct shear tests increased 3 to 10° as a result of compost treatment. Effective cohesion of the blends (16 to 18 kPa) were higher than that of topsoil (11 kPa) and the composts (8 kPa). Compaction at w_{opt+5} decreased the effective friction angles of topsoil, leaf compost, and leaf compost-topsoil blends by 2-6°, and increased the those of biosolids and biosolids-topsoil blends by 2-3°. Compost addition resulted in a 0-15° increase in effective friction angle of topsoil measured in CU triaxial shear tests. Total cohesion and friction angle of topsoil changed very little by compost treatment (by 0-8 kPa and 0-3°, respectively).

2) Factors of safety of the 7 and 12 m-high slopes ranged between 1.73 and 2.43 and between 2.73 and 3.54 for saturated and unsaturated conditions, respectively, indicating that a 5 cm-thick compost layer placed for vegetative growth would not pose any danger to overall stability of the highway slopes.
3) Digital image analyses indicated that the topsoil particles had lower angularity, flatness and elongation, and higher sphericity and smoothness, compared to those of biosolids and leaf composts. Angularity and Form 2D of all materials tested yielded higher R^2 (0.891-0.898 and 0.796-0.938, respectively) as compared to texture, flatness, elongation, and sphericity (0.345-0.864).
4) Saturated hydraulic conductivity (K_S) of topsoil increased from 1.2 x 10^{-7} cm/s to 1.7-5.5 x 10^{-6} cm/s as a result of compost treatment. Increasing the compaction water content by 5% beyond optimum water content decreased the K_S of materials by 1.3 (L) to 4 (TB1) times. K_S was strongly correlated with compost content, and gravel, sand, and fines contents. Material particle size had considerable effects on K_S, and, in particular, finer sizes, D_{10}, D_{30}, played a major role on hydraulic conductivity.
5) Biosolids and leaf compost had the plant available water contents (AWC) of 31.6 and 36.4%, respectively, compared to a value of 10.9% for topsoil. Compost amendment increased the AWC of T by approximately 1.4-2.6 times, potentially improving vegetative growth on highway slopes.
6) Unsaturated hydraulic conductivities of topsoil, composts, and the blends were comparable at the matric potential of field capacity (10 kPa). Decrease in hydraulic conductivity during the drying process was the sharpest on composts,

due to their high porosity and tortuosity. Biosolids and leaf compost treatments caused 1-3 orders of decreases in unsaturated hydraulic conductivity throughout the drying process.

4.2 Limitations of the Study and Recommendations for Future Research

The effects of compost treatment on shear and hydraulic properties of topsoil provided in this research study may help practitioners with regard to stability of highway slopes as well as infiltration, seepage, runoff, and vegetation establishment potential on these slopes. However, it should be recognized that the research findings are limited to one topsoil, two types of composts, and their select blends (15 and 30% by dry weight of compost) prepared following the textural and grading analyses requirements of the Maryland Department of Transportation State Highway Administration.

Past research has shown that compost increases the porosity and decreases the bulk density of the medium, which can lead to high infiltration rates but also high nutrient load (extractions of nitrogen, phosphorus, and potassium). The findings of the current study focused on physical characteristics of compost, and no tests were conducted to assess the nutrient leaching performance. It is strongly advised to run such leaching tests before incorporating compost into highway slopes.

Moreover, further tests can be performed with a variety of topsoil, compost, and blends to generalize the findings on shear and hydraulic conductivity. Chemical behavior (e.g., organic matter, fiber content, mineralogical composition) of different composts and compost-amended topsoils and their relationship to geotechnical properties should be further investigated. Lastly, large-scale laboratory model studies

and field studies need to be conducted to better understand compost addition on slope failure, runoff occurrence, infiltration, and vegetation establishment under varying climatic conditions.

Appendices

Appendix A

MDOT SHA Specifications for Topsoils

Table A1. Maryland Department of Transportation State Highway Administration – Special Provision Insert 920 – Landscaping Materials: Section 920.01.02 Furnished Topsoil, 2018

Composition - Furnished Topsoil					
Test Property	**Test [1] Method**	**Test Value and Amendment**			
Prohibited Weeds	—	Free of live stems and roots of species in 920.01.01 as well as live stems and roots of Bermudagrass, Quackgrass, and Yellow Nutsedge.			
Debris	—	920.01.01			
Grading Analysis	R-58	920.01.01			
Textural Analysis	T-88	**Particle**		**% Passing by Weight**	
		Size	**mm**	**Minimum**	**Maximum**
		Sand	2.0 – 0.050	20	75
		Silt	0.050 – 0.002	Combined Silt and Clay 25	75
		Clay	less than 0.002		30
Soil pH	ASTM D 4972	pH 6.1 to pH 7.2			
Organic Matter	T-267	4.0 to 8.0% OM by weight			
Nutrient Content	—	920.01.01			
Soluble Salts	EC 1:2 (V:V)	500 ppm (0.78 mmhos/cm) or less.			
Harmful Materials	—	920.01.01			

Note:
[1] Materials Standards and Materials Testing 356 (MSMT 356) has been superseded by OMT Landscaping Soils Eligibility List.
Test methods not defined herein shall be as per visual inspection or methods defined by the Landscape Operations Division.

Table A2. Maryland Department of Transportation State Highway Administration – Special Provision Insert 920 – Landscaping Materials: Section 920.01.02 Existing & Salvaged Topsoil, 2018

Composition – Existing Topsoil & Salvaged Topsoil					
Test Property	**Test[1] Method**	**Test Value and Amendment**			
Prohibited Weeds	—	Free of live stems or roots of Shattercane, Johnsongrass, Canada Thistle, Bull Thistle, Plumeless Thistle, Musk Thistle, Common Reed and Japanese Knotweed when inspected before transportation.			
Debris	—	1.0 % or less by weight of cement, concrete, asphalt, crushed gravel or construction debris when inspected.			
Grading Analysis	R-58	**Sieve Size**		**Passing by Weight Minimum %**	
		2 in.		100	
		No. 4		90	
		No. 10		80	
Textural Analysis	T-88	**Particle**		**% Passing by Weight**	
		Size	**mm**	**Minimum**	**Maximum**
		Sand	2.0 – 0.050	15	77
		Silt	0.050 – 0.002	Combined Silt and Clay 23	80
		Clay	less than 0.002		30
Soil pH	ASTM D 4972	pH of 4.8 to 7.6. Apply limestone to Existing Topsoil and Salvaged Topsoil with pH 4.8 to 6.1 per NMP. Apply sulfur to Existing Topsoil and Salvaged Topsoil with pH 7.1 to 7.6 per NMP.			
Organic Matter	T-267	1.0 to 8.0 % OM by weight. Apply compost to Existing Topsoil and Salvaged Topsoil with 1.0 to 3.7% OM per NMP.			
Nutrient Content	—	Administration will assess. Apply fertilizer per NMP for nitrogen requirement and optimum fertility index values (FIV) for phosphorus and potassium.			
Soluble Salts	EC 1:2 (V:V)	800 ppm (1.25 mmhos/cm) or less. Apply gypsum to Existing Topsoil and Salvaged Topsoil with 500 to 800 ppm (0.78 to 1.25 mhos/cm) per NMP.			
Harmful Materials	—	Topsoil shall not contain substances in concentrations that are harmful to human health, water quality, or plant growth. Industrial waste such as ash, slag, raw sludge, dredge spoil, or similar materials shall not be soil components.			

Note:
[1] Materials Standards and Materials Testing 356 (MSMT 356) has been superseded by OMT Landscaping Soils Eligibility List.
Test methods not defined herein shall be as per visual inspection or methods defined by the Landscape Operations Division.

Table A3. Parameters for the topsoil, compost and the blends measured in the current study, and their comparison with the MDOT SHA Specification – Section 920.01.02 for Existing/Salvaged and Furnished Topsoils (2018).

Legend	Composition	Parameter	Average Value	Range in the MDOT SHA Specifications	Meets limits?
T	100% topsoil	OM (%)	4.39 ± 0.193	4-8	Yes
		pH	6.9 ± 0.071	4.8-7.6	Yes
		Size	Sand=47.3%; Silt=37.4%; Clay=4.9%	See Tables A1 and A2	Yes
B	100% biosolids compost	OM (%)	60.55 ± 0.781	4-8	**No**
		pH	5.5 ± 0.022	4.8-7.6	Yes
		Size	Sand=48.6%; Silt=4.3%; Clay=0.2%	See Tables A1 and A2	**No**
L	100% leaf compost	OM (%)	61.57 ± 0.071	4-8	**No**
		pH	7.9 ± 0.058	4.8-7.6	**No**
		Size	Sand=72.5%; Silt=8.0%; Clay=0.2%	See Tables A1 and A2	**No**
TB1	85% topsoil+15% biosolids compost	OM (%)	13.95 ± 0.714	4-8	**No**
		pH	6.2 ± 0.105	4.8-7.6	Yes
		Size	Sand=45.9%; Silt=32.7%; Clay=4.2%	See Tables A1 and A2	Yes
TB2	70% topsoil+30% biosolids compost	OM (%)	17.20 ± 0.569	4-8	**No**
		pH	6.0 ± 0.142	4.8-7.6	Yes
		Size	Sand=44.1%; Silt=27.4%; Clay=3.5%	See Tables A1 and A2	Yes
TL1	85% topsoil+15% leaf compost	OM (%)	16.14 ± 0.865	4-8	**No**
		pH	7.5 ± 0.065	4.8-7.6	Yes
		Size	Sand=51.1%; Silt=33.0%; Clay=4.2%	See Tables A1 and A2	Yes
TL2	70% topsoil+30% leaf compost	OM (%)	19.03 ± 0.318	4-8	**No**
		pH	7.6 ± 0.034	4.8-7.6	Yes
		Size	Sand=58.3%; Silt=25.7%; Clay=3.0%	See Tables A1 and A2	Yes

Appendix B

Compaction and Direct Shear Tests

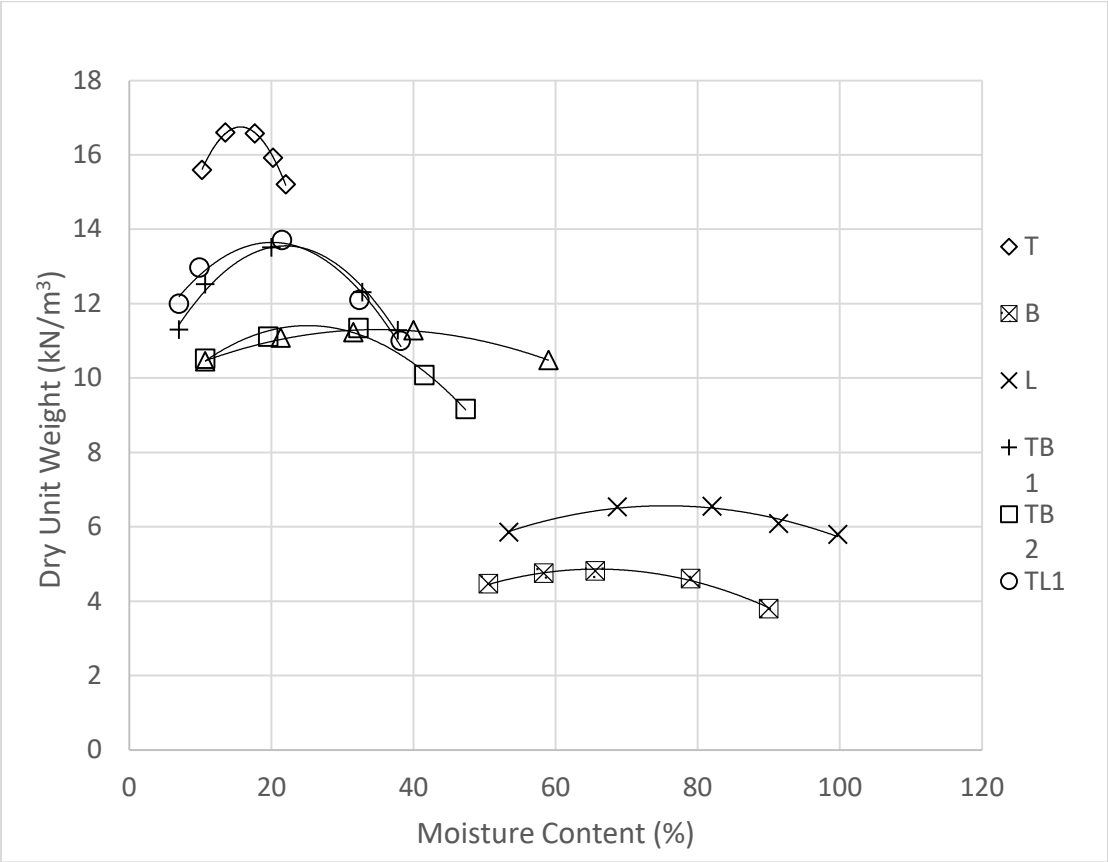

Figure B1. Compaction Curves of Materials Tested

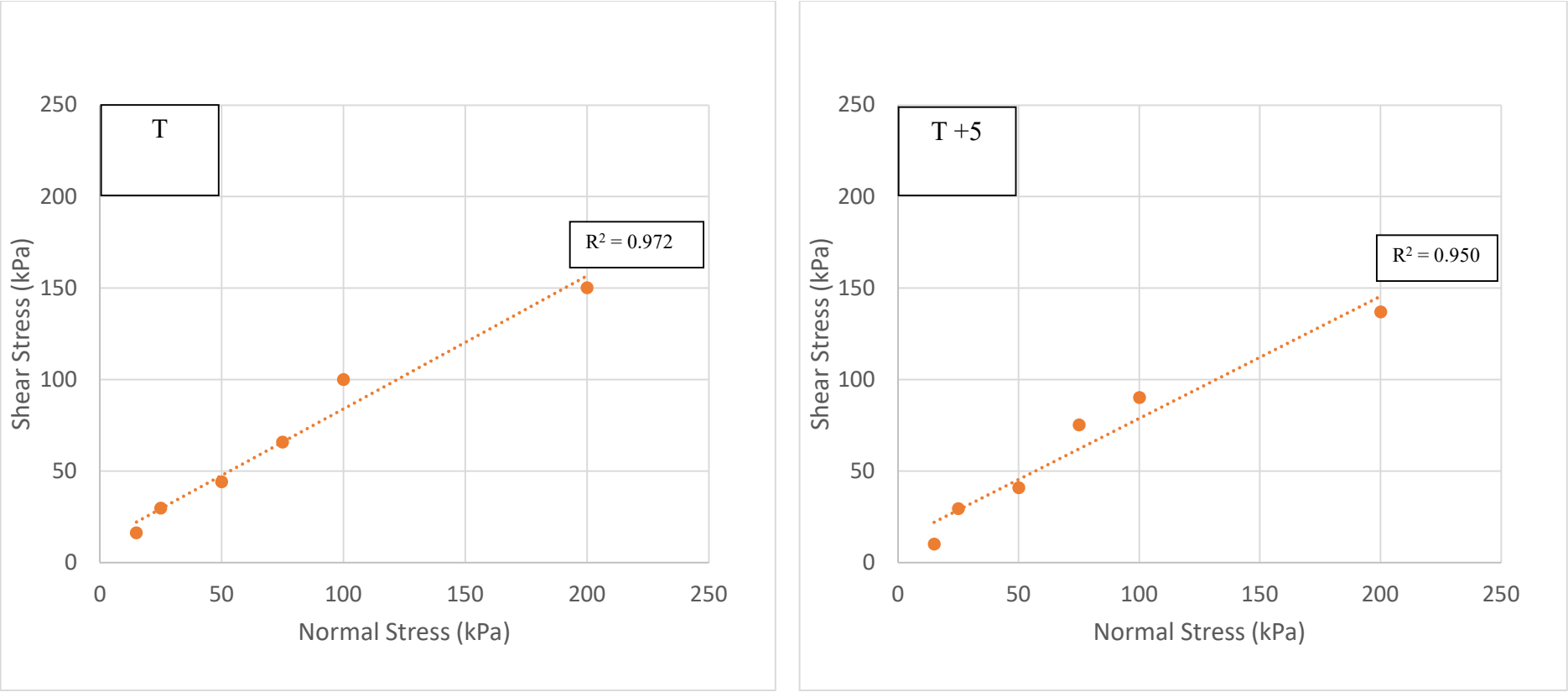

Figure B2. Direct shear results of the materials tested

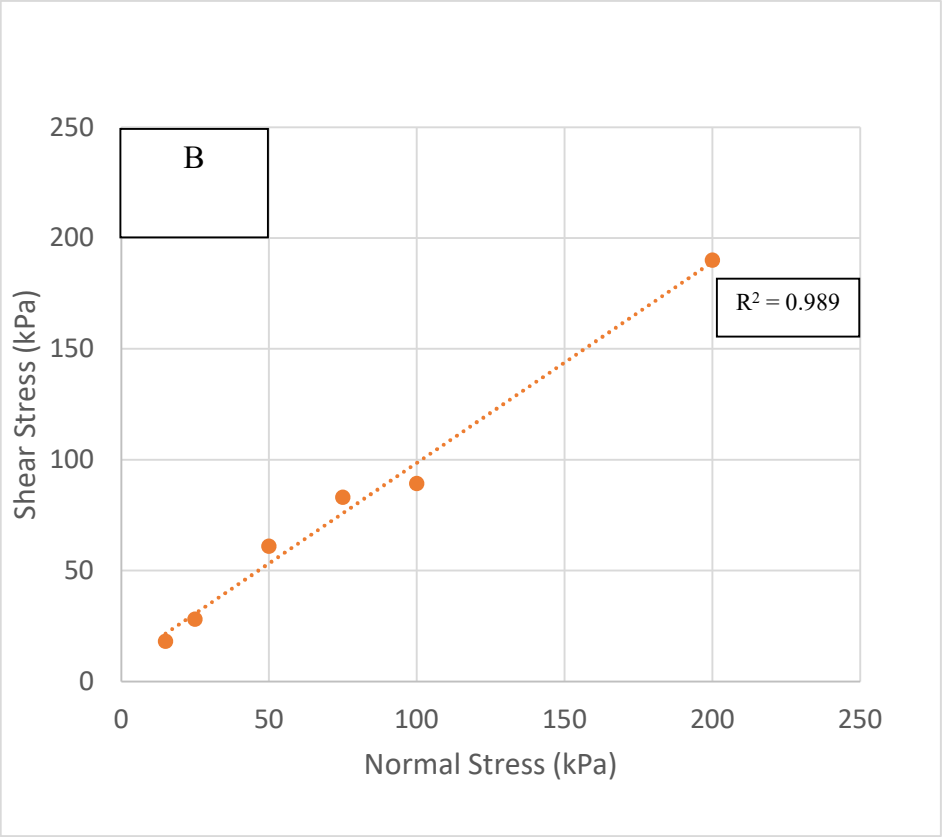

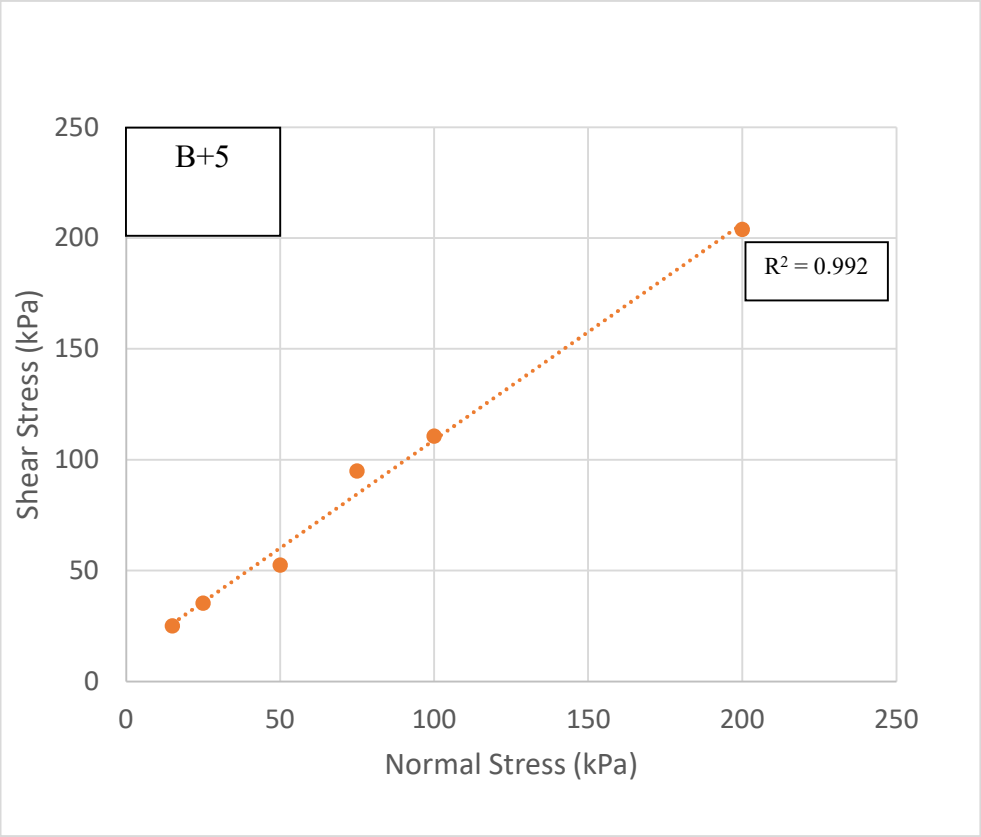

Figure B2 (cont'd). Direct shear results of the materials tested

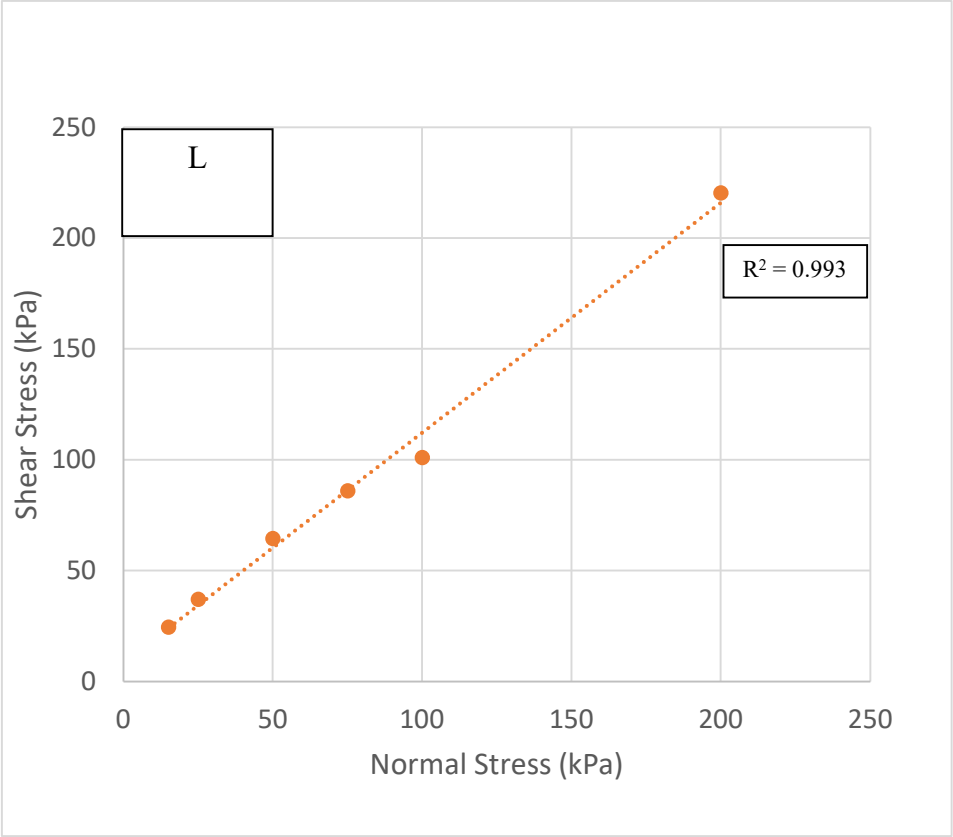

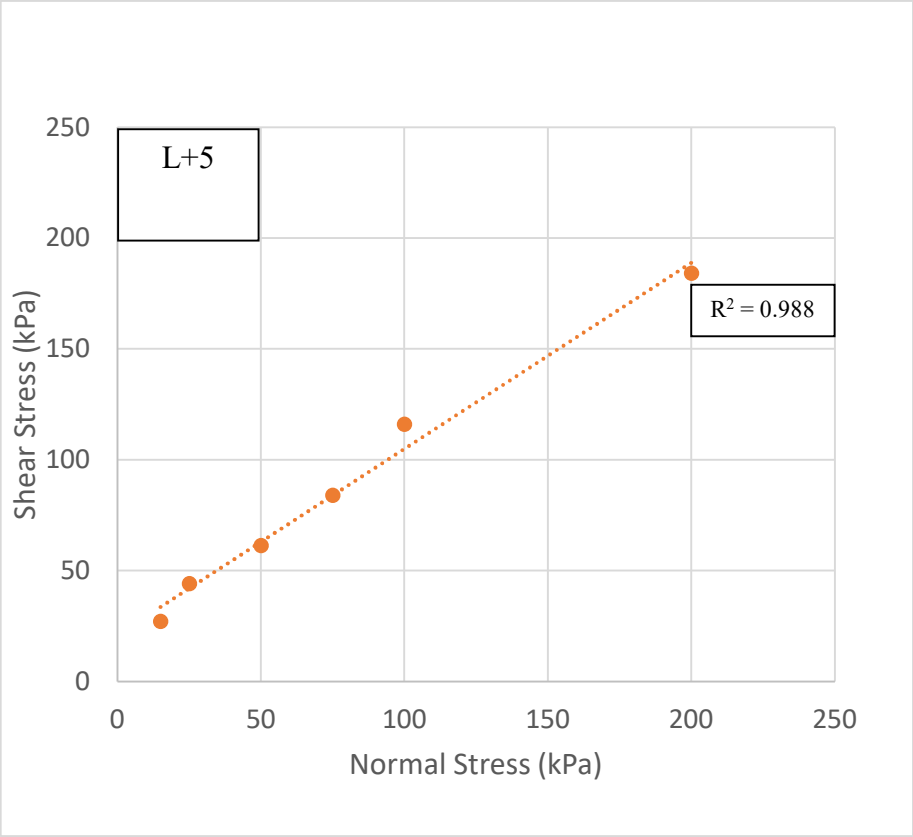

Figure B2 (cont'd). Direct shear results of the materials tested

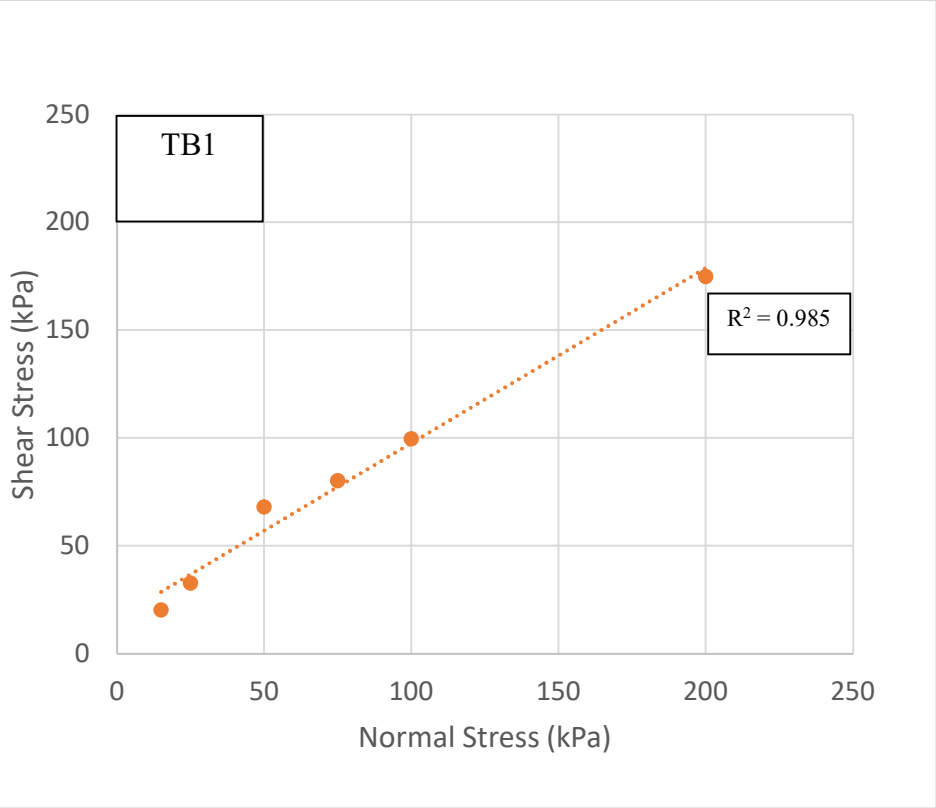

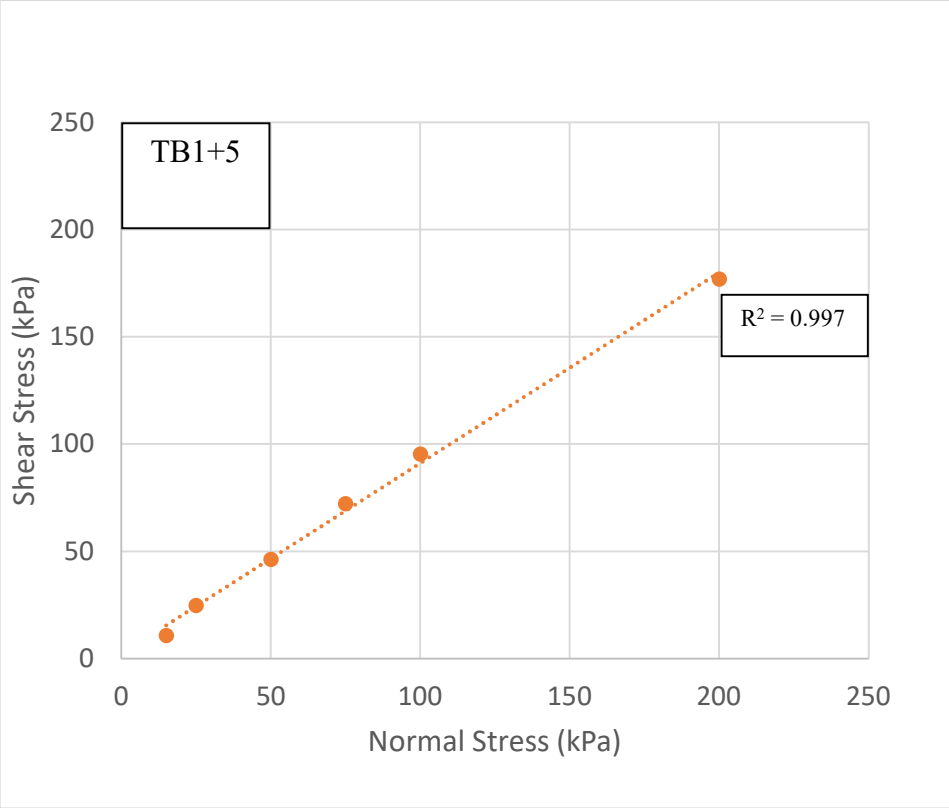

Figure B2 (cont'd). Direct shear results of the materials tested

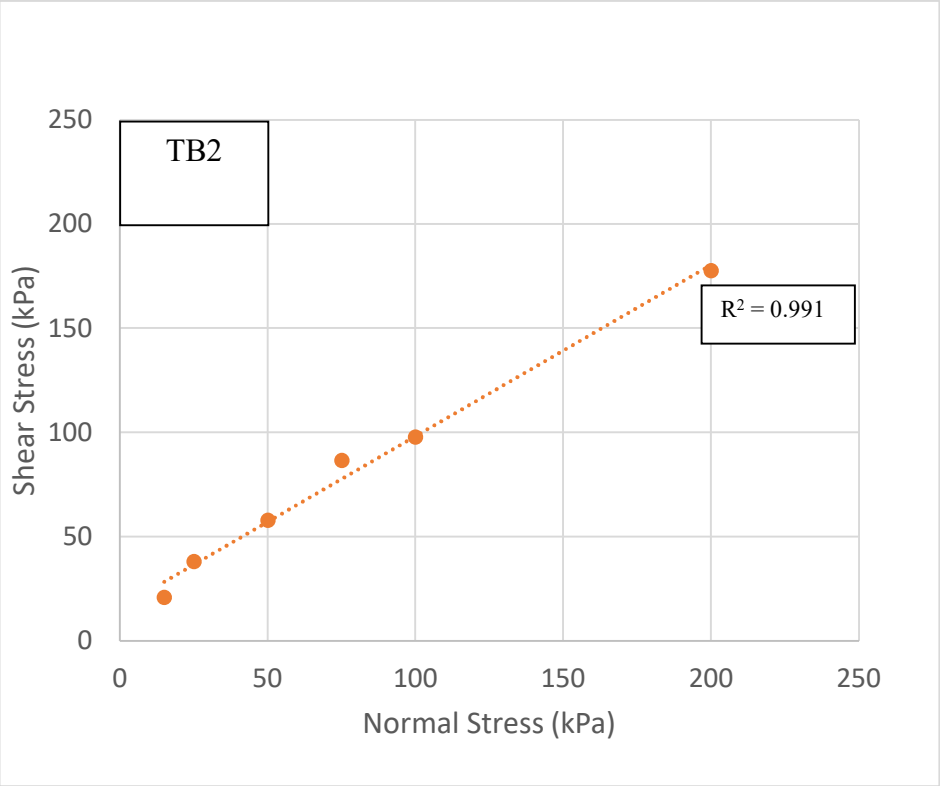

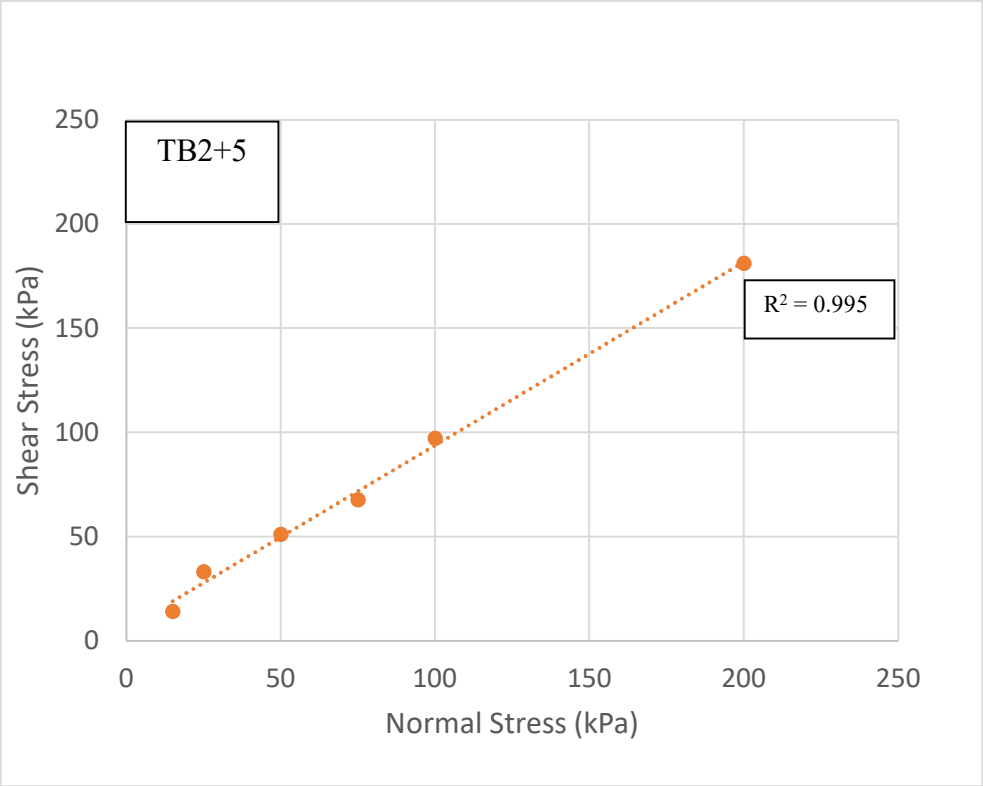

Figure B2 (cont'd). Direct shear results of the materials tested

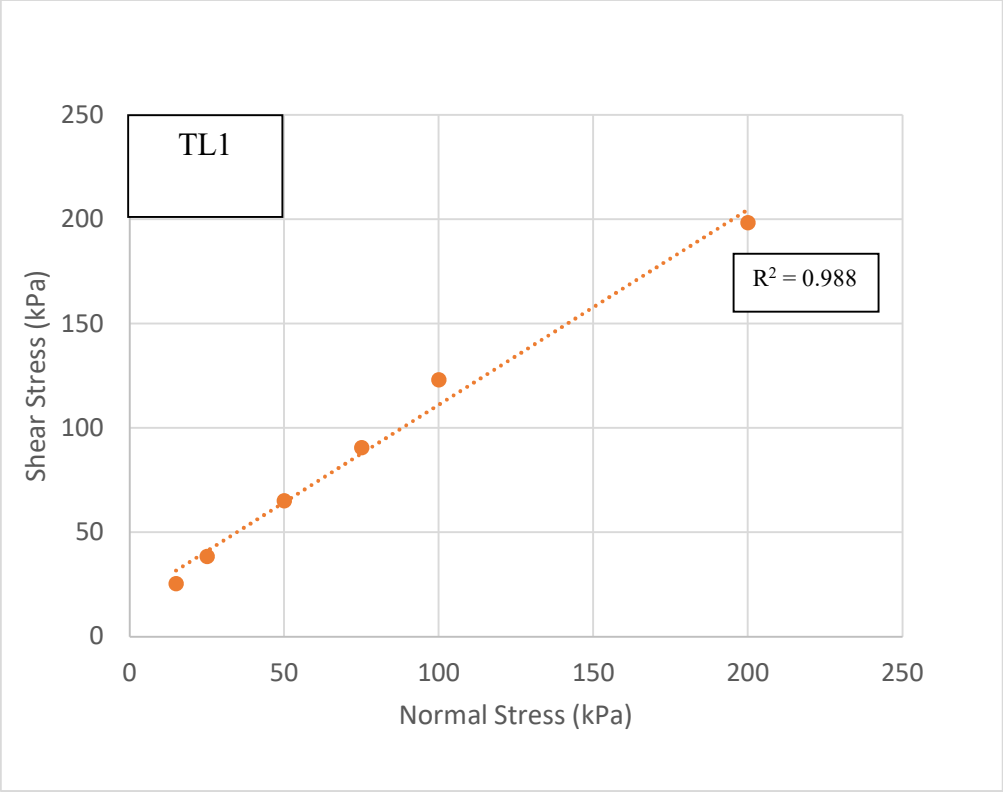

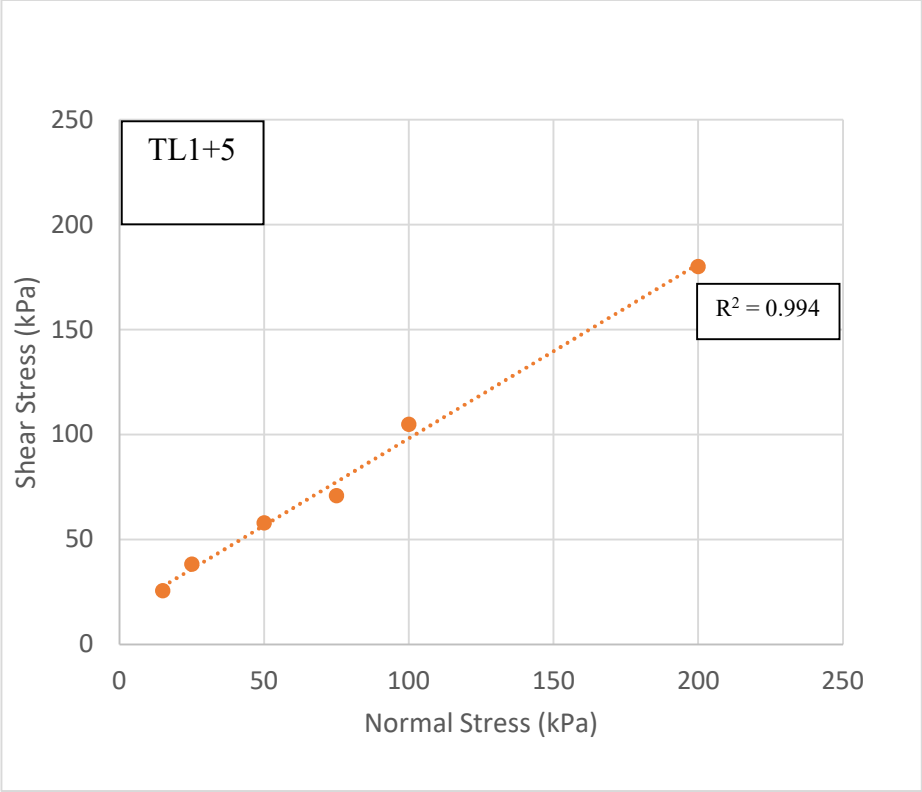

Figure B2 (cont'd). Direct shear results of the materials tested

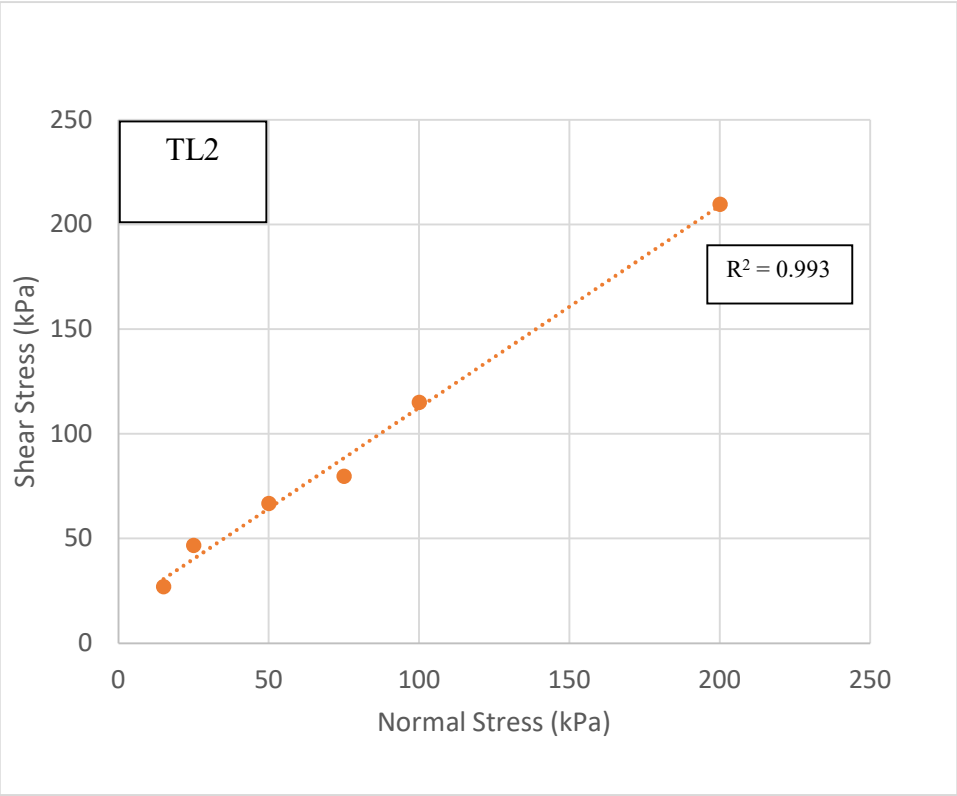

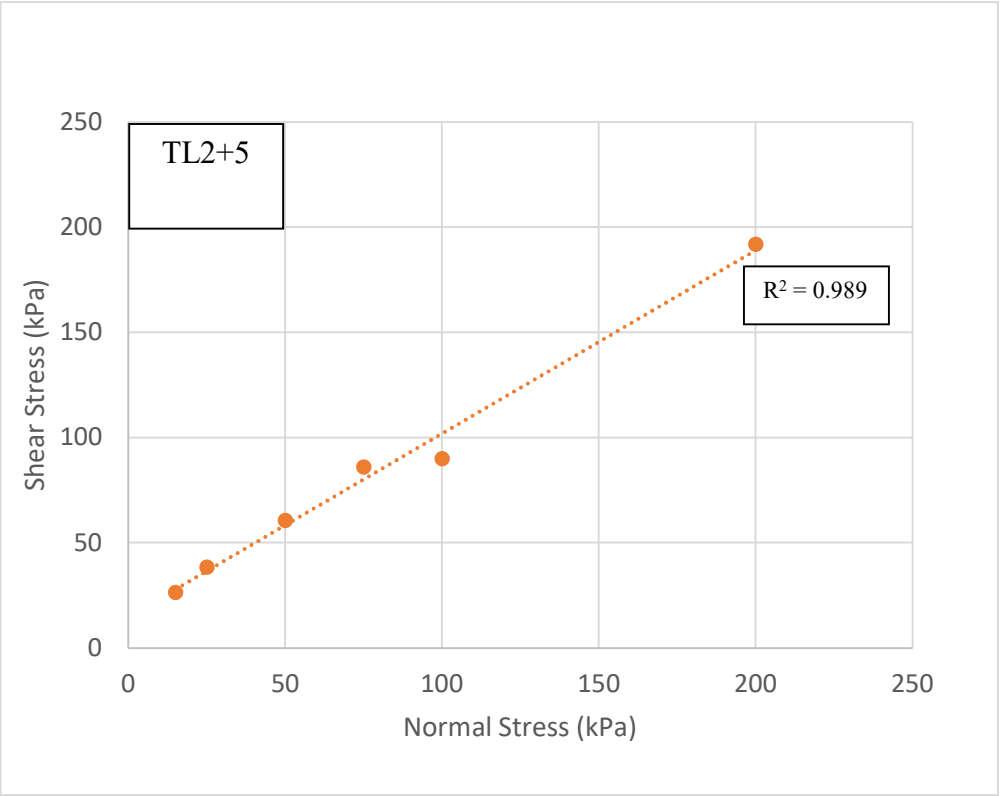

Figure B2 (cont'd). Direct shear results of the materials tested

Appendix C

AIMS Analysis and Parametric Studies

Table C1. Particle ranges for each analysis

<table>
<tr><th>Analysis</th><th colspan="4">Particle Range</th></tr>
<tr><td>Angularity</td><td>> 4.75 mm</td><td>4.75 – 2.00 mm</td><td>2.00 – 0.6 mm</td><td>0.6 – 0.075 mm</td></tr>
<tr><td>Form 2D</td><td>4.75 – 2.00 mm</td><td>2.00 – 0.6 mm</td><td colspan="2">0.6 – 0.075 mm</td></tr>
<tr><td>Texture</td><td colspan="4">> 4.75 mm</td></tr>
<tr><td>Sphericity</td><td colspan="4">> 4.75 mm</td></tr>
<tr><td>Flatness</td><td colspan="4">> 4.75 mm</td></tr>
<tr><td>Elongation</td><td colspan="4">> 4.75 mm</td></tr>
</table>

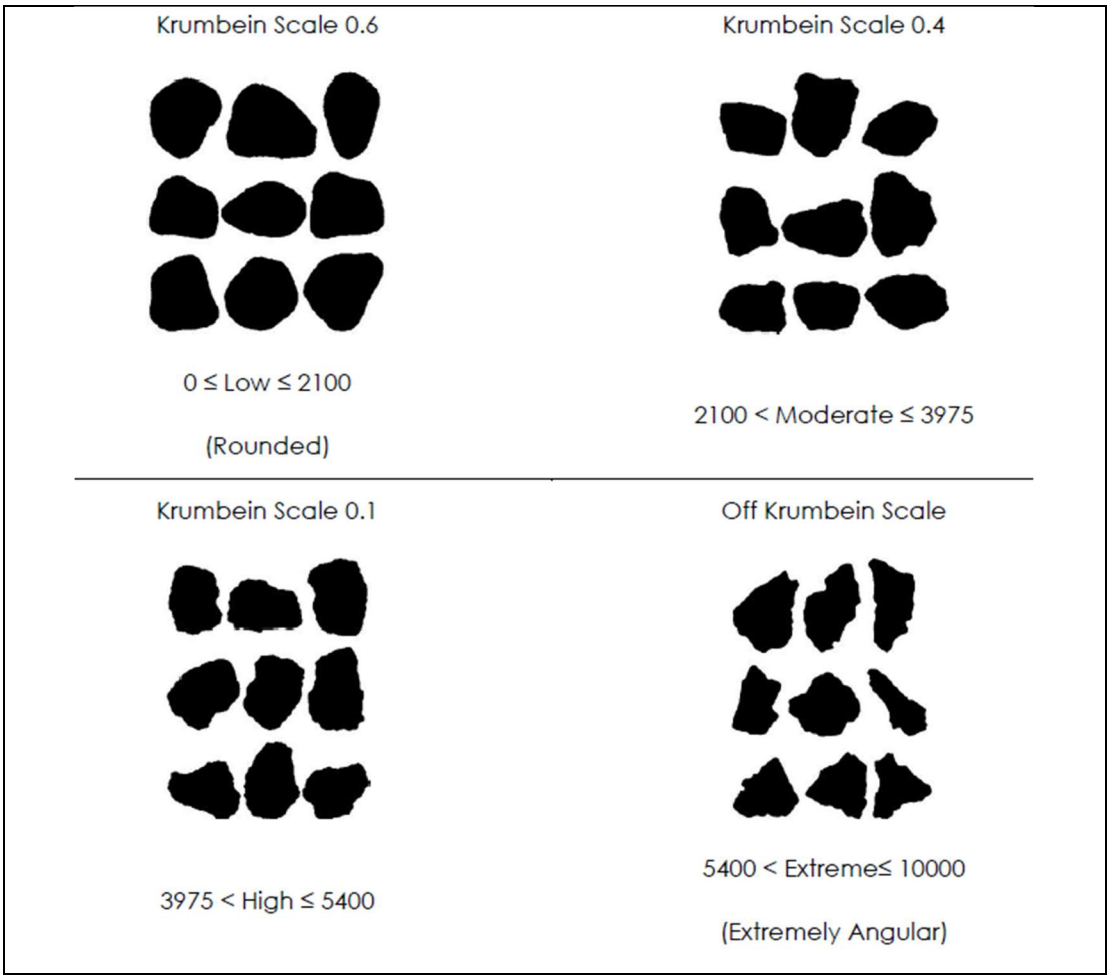

Figure C1. Angularity Range of AIMS (by AIMS-Manual, 2017)

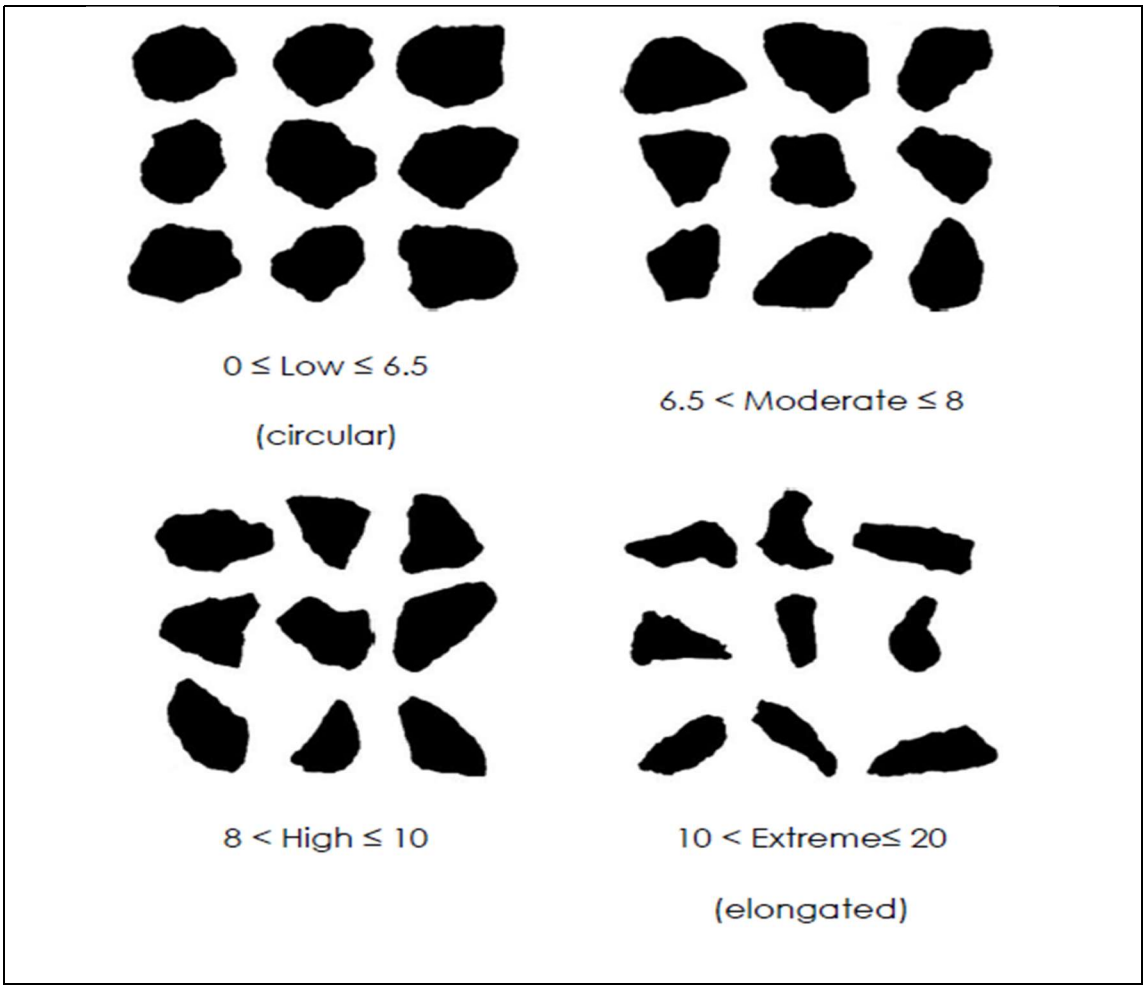

Figure C2. Form 2D range of AIMS (by AIMS-Manual, 2017)

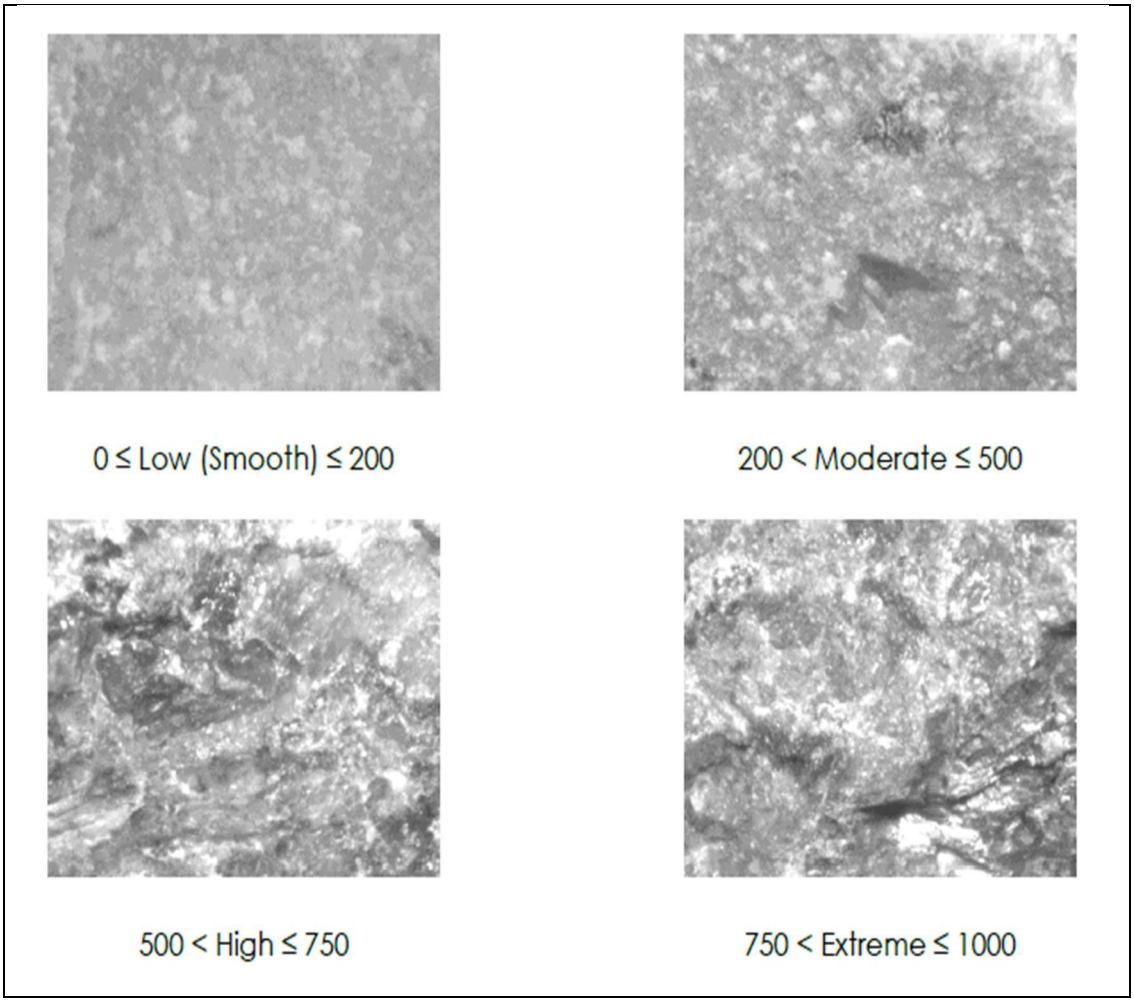

Figure C3. Texture range of AIMS (by AIMS-Manual, 2017)

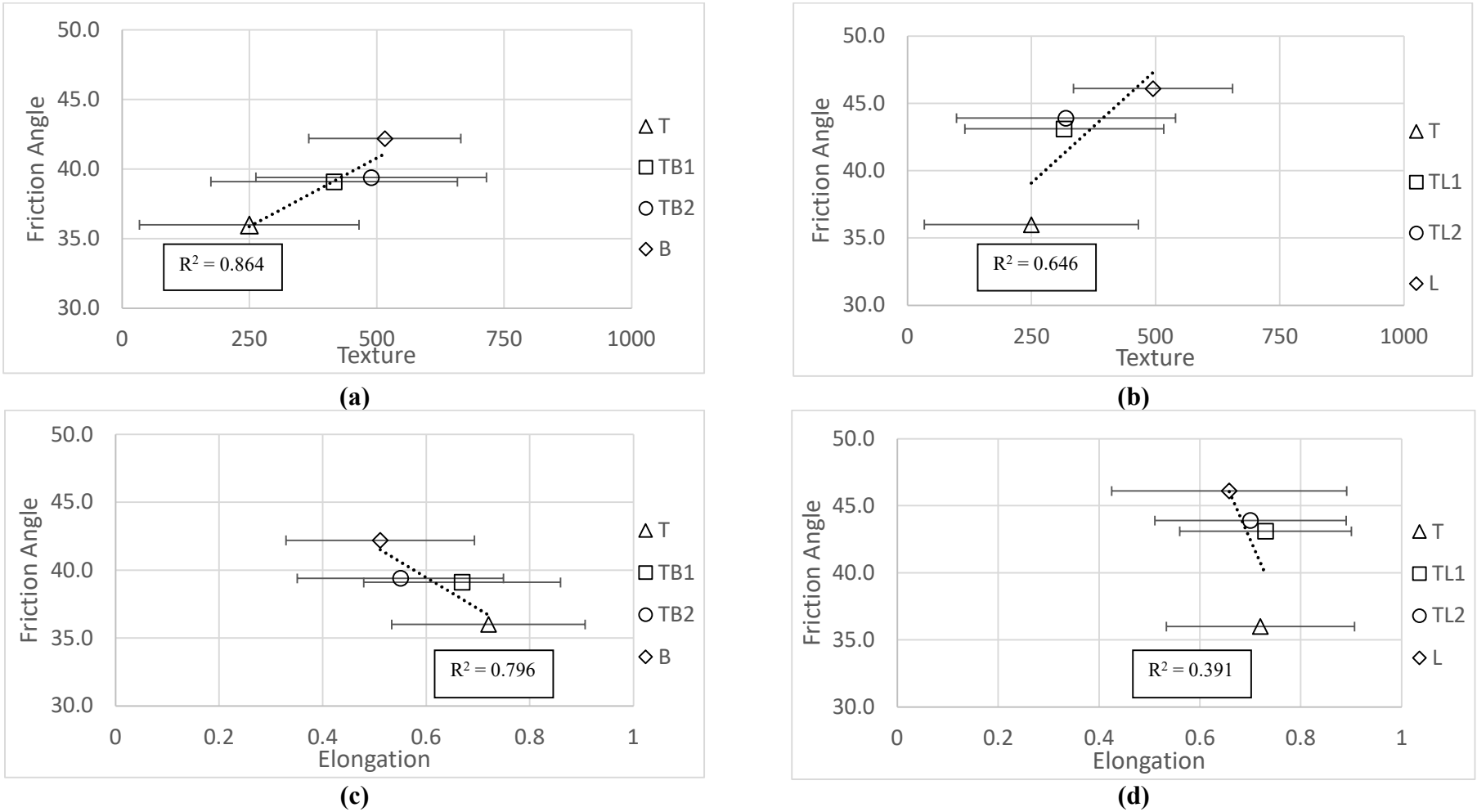

Figure C4. Correlation between texture and friction angle by (a) B and (b) L amendment, and between the elongation and friction angle by (c) B and (d) L amendment

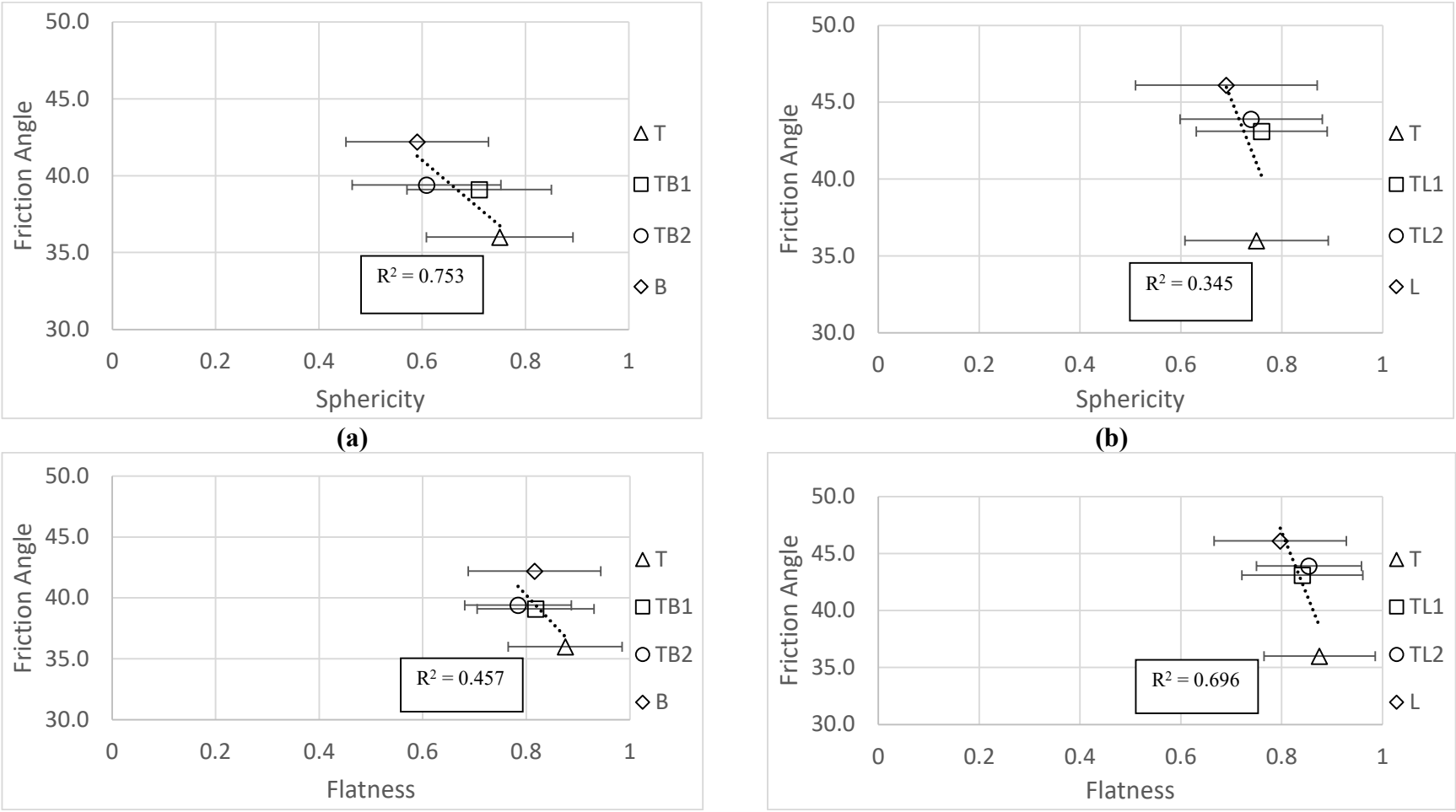

Figure C5. Correlation between sphericity and friction angle by (a) B and (b) L amendment, and between the flatness and friction angle by (c) B and (d) L amendment

Figure C6. Two leaf compost particles with the same particle range (> 4.75-mm) but different shape

References

Adugna, G. 2016. "A review on impact of the compost on soil properties, water use and crop productivity." *Academic Research Journal of Agricultural Science and Research* 4 (3): 93-104. https://doi.org/10.14662/ARJASR2016.010.

Al-Riffai, M. 2005. "Adopting unsaturated flow properties in the design of earthen dams: an integrated design approach to hydrologic and geotechnical events." *1st Conference on Unsaturated Soils*, Ottawa, ON. https://doi.org/10.13140/2.1.3927.2329.

Bajwa, T. M., and Fall, M. 2011. "Mechanical characteristics and behavior of compost-based landfill cover." In *Proc., Pan-Am CGS Geotechnical Conf., No. 577.* Richmond, BC, Canada: Canadian Geotechnical Society.

Bezerra-Coelho, C. R., Zhuang, L., Barbosa, M. C., Soto, M. A., and Genuchten, M. T. V. 2017. "Further tests of the HYPROP evaporation method for estimating the unsaturated soil hydraulic properties." *J. Hydrol. Hydromech*. 66: 161–169. https://doi.org/10.1515/johh-2017-0046.

Chaganti, V. N., Crohn, D. M. 2014. "Evaluation of compost blankets for erosion control and runoff water quality on a constructed hillslope in Southern California." *Trans. ASABE* 57 (2): 403–416. https://doi.org/10.13031/trans.57.10199.

Cho, G. C., Dodds, J., and Santamarina, J. C. 2006. "Particle shape effects on packing density, stiffness, and strength: natural and crushed sands." *J. Geotech. Geoenviron. Eng.* 132: 591–602. https://doi.org/10.1061/(ASCE)1090-0241(2006)132:5(591).

Colman, E. A. 1947. "A laboratory procedure for determining the field capacity of field soils." *Soil Sci.* 63: 277-283.

Eghball B, D. Ginting, and J. E .Gilley. 2004. "Residual effects of manure and compost applications on corn production and soil properties." *Agronomy Journal* 96: 442- 447. https://doi.org/10.2134/agronj2004.0442.

Faucette, B., Risse, M. 2002. "Water quality impacts: controlling erosion with compost and mulch." *Biocycle* June: 26-28.

Faucette, L. B., C. F. Jordan, L. M. Risse, M. Cabrera, D. C. Coleman, and L. T. West. 2005. "Evaluation of storm water from compost and conventional erosion control practices in construction activities." *Journal of Soil and Water Conservation* 60 (6): 288-297. https://doi.org/10.1007/b100570.

Faucette, L. B., Governo, J., Jordan, C. F., Lockaby, B. G., Carino, H. F., and Governo, R. 2007. "Erosion control and storm water quality fromstraw with PAM, mulch, and compost blankets of varying particle sizes." *Journal of Soil and Water Conservation* 62 (6): 404-413.

Faucette, L. B., B. Scholl, R. E. Bieghley, and J. Governo. 2009. "Large-scale performance and design for construction activity erosion control best management practices." *Journal of Environmental Quality* 38: 1248–1254. https://doi.org/10.2134/jeq2008.0415.

Federal Highway Administration. 2004. "Transportation applications of recycled concrete aggregate." *FHWA State of the Practice National Review*, FHWA, Washington, DC.

Gonzalez, R. F., and Cooperband, L. R. 2002. "Compost effects on soil physical properties and field nursery production." *Compost Science & Utilization* 10: 226–237. https://doi.org/10.1080/1065657X.2002.10702084.

Harrison, R. B. 2008. "Composting and formation of humic substances." *Encyclopedia of Ecology* 713-719. https://doi.org/10.1016/B978-008045405-4.00262-7.

Hartl, W., and Erhart, E. 2005. "Crop nitrogen recovery and soil nitrogen dynamics in a 10-year field experiment with biowaste compost." *J. Plant Nutr. Soil Sci.* 168: 781-788. https://doi.org/10.1002/jpln.200521702.

Hatipoglu, M., Cetin, B., and Aydilek, A. H. 2020. "Effect of fines content on the performance of unbound granular base aggregates." *Journal of Transportation, Part B: Pavements*, ASCE, 146 (1). https://doi.org/10.1061/JPEODX.0000141.

Hosea, T., Cougnonb, M. De Vlieghera, A., Van Bockstaele, E., and Reheul, D. 2012. "Influence of farm compost on soil quality and crop yields." *Archives of Agronomy and Soil Science* 58: 71-75. https://doi.org/10.1080/03650340.2012.692876.

Hubbert, M. K. 1940. "The theory of groundwater motion." *J Geol.* 48 (8): 785–944. https://doi.org/10.1029/TR021i002p00648-1.

Huntington, T. G. 2007. "Available water capacity and soil organic matter." *Encyclopedia of soil science. New York: Taylor and Francis* 139–143.

Intharasombat, N. 2005. "Laboratory and field investigations to address erosion, volume change and desiccation cracking of compost amended expansive subsoils." Ph.D. Dissertation, The University of Texas at Arlington.

Intharasombat, N., Puppala, A. J., and Williammee, R. 2007. "Compost amended soil treatment for mitigating highway shoulder desiccation cracks." *Journal of Infrastructure Systems* 13 (4): 287–298. https://doi.org/10.1061/(ASCE)1076-0342(2007)13:4(287).

Jamison, V. C., and E. M. Kroth. 1958. "Available moisture storage capacity in relation to textural composition and organic matter content of several Missouri Soils1." *Soil Sci. Soc. Am. J.* 22 (3): 189-192. https://doi.org/10.2136/sssaj1958.03615995002200030001x.

Jennings, S. R., J. D. Goering, P. S. Blicker, and J. J. Taverna. 2003. "Evaluation of organic matter addition and incorporation on steep cut slopes phase I: Literature review and potential application equipment evaluation." Montana Department of Transportation Research Program, Helena MT.

Kirchoff, C., Malina, J., and Barrett, M. 2003. "Characteristics of compost: moisture holding and water quality improvement." *Center for Research in Water Resources.* 1-4.

Kirkham, M. B. 2005. "Principles of soil and plant water relations." *Burlington: Academic Press* 500.

Koerner, M. R. 1970. "Effect of particle characteristics on soil strength." *Journal of Soil Mechanics and Foundation Division*, ASCE, 96 (SM4): 1221–1234.

Le, M., Puppala, A. J., and Pedarla, A. 2015. "Effect of compost soil treatment on surficial slope stability in fully softened condition." *Geotechnical Special Publication* 2748-2757. https://doi.org/10.1061/9780784479087.256.

Maynard, A. A., and D. E. Hill. 1994. "Impact of compost on vegetable yields." *BioCycle* 35 (3): 66-67.

Minasny, B., and McBratney, A. B. 2018. "Limited effect of organic matter on soil available water capacity." *Eur. J. Soil Sci.* 69: 39–47. https://doi.org/10.1111/ejss.12475.

Mualem, Y. 1976. "A new model for predicting the hydraulic conductivity of unsaturated porous media." *Water Resour. Res.* 12: 513–522. https://doi.org/10.1029/WR012i003p00513.

Mukhtar, S., M. McFarland, C. Gerngross, and F. Mazac. 2004. "Efficacy of using dairy manure compost as erosion control and revegetation material." *American Society of Agricultural Engineers/Canadian Society of Agricultural Engineers Annual International Meeting*, Ontario, CA. Paper No. 44079. https://doi.org/10.13031/2013.16786.

Olanrewaju, J. N., and Wong, T. 1994. "Hydraulic conductivity, porosity, and particle size distribution of core samples of the upper glacial aquifer: Laboratory observations." State Univ. of New York at Stony Brook, Stony Brook, NY, 73–79.

Pertassek, T., Peters, A., and Durner, W. 2011. "HYPROP data evaluation software user's manual, V.1.0." UMS GmbH, Gmunder Str. 37, 81379 München, Germany.

Platt, B., Bell, B., and Harsh, C. 2013. "Pay dirt: composting in Maryland to reduce waste, create jobs & protect the Bay.", *ILSR*.

Puppala, A. J., Banavathu, N., Qasim, S. R., Williammee, R., and Intharasombat, N. 2004. "Laboratory investigation to address the use of compost amendments to enhance expansive subsoils." *In: Recycled materials in geotechnics sessions at ASCE civil engineering conference and exposition,* ASCE. https://doi.org/10.1061/40756(149)6.

Puppala, A. J., S. P. Pokala, N. Intharasombat, and R. Williammee. 2007. "Effects of organic matter on physical, strength, and volume change properties of compost amended expansive clay." *J. Geotech. Geoenviron. Eng*. 133: 1449-1461. https://doi.org/10.1061/(ASCE)1090-0241(2007)133:11(1449).

Ratliff, L. F., J. T. Ritchie, and D. K. Cassel. 1983. "Field-measured limits of soil water availability as related to laboratory-measured properties1." *Soil Sci. Soc. Am. J.* 47: 770-775. https://doi.org/10.2136/sssaj1983.03615995004700040032x.

Schindler, U., von Unold, G., Durner, W., and Müller, L. 2010a. "Evaporation method for measuring unsaturated hydraulic properties of soils: extending the range." *Soil Sci. Soc. Am. J.* 74: 1071–1083. https://doi.org/10.2136/sssaj2008.0358.

Shinohara, K., Oida, M., and Golman, B. 2000. "Effect of particle shape on angle of internal friction by triaxial compression test." *Powder Technol* 107: 131–136. https://doi.org/10.1016/S0032-5910(99)00179-5.

Shinomiya, Y., K. Takahashi, M. Kobiyama, and J. Kubota. 2001. "Evaluation of the tortuosity parameter for forest soils to predict unsaturated hydraulic conductivity." *J. For. Res*. 6: 221–225. https://doi.org/10.1007/BF02767097.

Siahdashti, M. J., Jean Côté, and Philippe Sirois. 2015. "Effect of grain size distribution on the hydraulic properties of unsaturated granite sand." In *15th Pan-American Conference on Soil Mechanics and Geotechnical Engineering.* https://doi.org/10.3233/978-1-61499-603-3-2180.

Sullivan, D. 2018. "Interpreting compost analyses." *Technical Report EM 9217*, Oregon State University.

Tokunaga, T. K. 2009. "Hydraulic properties of adsorbed water films in unsaturated porous media." *Water Resources Research* 45: W06415. https://doi.org/10.1029/2009WR007734.

Veeresh, H., S. Tripathy, D. Chaudhuri, B. C. Ghosh, B. R. Hart, and M. A. Powell. 2003. "Change in physical and chemical properties of three soil types in India as a result of amendment with fly ash and sewage sludge." *Environmental Geology* 43: 513–520. https://doi.org/10.1007/s00254-002-0656-2.

Vereecken, H., Weynants, M., Javaux, M., Pachepsky, Y., Schaap, M. G., and van Genuchten, M. T. 2010. "Using pedotransfer functions to estimate the van Genuchten–Mualem soil hydraulic properties: a review." *Vadose Zone J*. 9: 795–820. https://doi.org/10.2136/vzj2010.0045.

Y. Li. 2013. "Effects of particle shape and size distribution on the shear strength behavior of composite soils." *Bull. Eng. Geol. Environ*. 72 (3–4): 371–381. https://doi.org/10.1007/s10064-013-0482-7.

Zare, M., Afyuni, M., and Abbaspour K. C. 2010. "Effects of biosolids application on temporal variations in soil physical and unsaturated hydraulic properties." *J Residuals Sci Technol*. 7 (4): 227–235.

Zhang, Z. F., A. L. Ward, and G. W. Gee. 2003. "A tensorial connectivity-tortuosity concept to describe the unsaturated hydraulic properties of anisotropic soils." *Vadose Zone J* 2: 313–321. https://doi.org/10.2113/2.3.313.

Zibilske, L., W. M. Claphamm, and R. V. Rourke. 2000. "Multiple applications of paper mill sludge in an agricultural system: soil effects." *J. Environ. Qual.* 29: 1975–1981. https://doi.org/10.2134/jeq2000.00472425002900060034x.